From Lagging to Leading: The Measured Emergence of Standing Capacitance Behind Consumer Connections, 1997–2025

D. J. Hume

***Abstract*—Both ENTSO-E Final Reports on the 2025 Iberian and North Macedonian blackouts read the excess capacitive reactive power as a network term—the reading the available data supports. The Iberian report asks for what was missing: information on load composition. We build that record from regulatory half-hourly metering at New Zealand's transmission–distribution boundary, spanning 29 years, and find a second source: the demand behind the customer's connection, at mains voltage and in residential, commercial and industrial premises alike, has itself moved capacitive. Overnight reactive power crossed from lagging to leading in 2016, nearly a decade before the 2025 events, and a first-principles charging calculation puts the demand-side share of that drift in the physical band 75–88%. That term behaves as a net standing shunt element—present around the clock, scaling with the connections served, and moving capacitive by about 230 VAr per connection over 2013–2025 and roughly 20 VAr a year at the close. It drives the drift rather than the level: the distribution network's own cable and line charging remains the larger part of the standing leading reactive power, and what changed is that a demand once strongly lagging stopped masking it. The candidate device layer is the electromagnetic-compatibility filter mandated in nearly every mains-connected product (a labelled hypothesis): a few VAr per device, tens of devices per household, millions across a system and perhaps billions on the largest—permanently across the mains and switched by nobody. Its injection rises with the square of mains voltage, so every 230-volt system accumulates about three times more per device than a 120-volt, 60-hertz one. Planning and protection studies still carry a constant lagging load archetype, where the overnight flow now has the opposite sign. Both inputs to the measurement are records any operator already holds.**

***Index Terms*—Reactive power, power factor, overvoltage, leading power factor, shunt capacitance, distribution cabling, measurement, grid exit point, load composition, load modelling, power-system analysis.**

I. Introduction

POWER systems internationally are shifting from net-absorbing (lagging) toward net-generating (leading) reactive power at light load, as the connected load fleet modernises toward power-electronic devices and networks add underground cabling. The direction of the transition is not in dispute, and this paper does not claim to be the first to observe it. What has been missing is, first, a long *measured* record of the transition observed end to end at supply-point resolution, and second, a measured separation of how much of the drift is the load fleet and how much is the network. This paper supplies both for a single national system, connects the result to a failure mode that has recently moved from theory to realised blackouts, and closes with what the reversal implies for the analysis and defences that were built for the opposite regime. The trail leads somewhere unexpected: to the electromagnetic-compatibility filter inside every mains-connected device—capacitance that one part of the regulatory apparatus requires and no other part counts—advanced here as a labelled hypothesis with its decisive test identified.

A. A global reactive transition, already observed

The phenomenon is well attested across jurisdictions. In Great Britain, Kaloudas *et al.* [1], [2] documented a steep decline in reactive demand at minimum load, with distribution networks beginning to export reactive power to the transmission system; in France, the transmission operator attributes off-peak overvoltage episodes to a three-factor mechanism of distributed generation, underground cabling, and evolving final consumption [3]; in Australia, Powerlink Queensland links a rising likelihood of overvoltage events partly to more energy-efficient appliances alongside rooftop solar [4]. Rising capacitive export to the extra-high-voltage network has likewise been reported in continental Europe [5]. At device level, Hannagan *et al.* [6] found the majority of modern household appliances present a leading power factor, and international expert reviews reach consistent conclusions about modern lighting and power electronics and about the error introduced by constant-power-factor load modelling [7], [8]. No consumer-device standard requires a unity fundamental-frequency (displacement) power factor: IEC 61000-3-2 limits harmonic current only [9], and a 2020 amendment removed the last power-factor term from its limits. The one device-level power-factor family in force anywhere—the European, and from 2026 Australian, lighting floors [10]—is a full-load, direction-blind metric that never sees a device's standing draw, and it has no New Zealand counterpart. The European Demand Connection Code remains the only international instrument addressing reactive exchange at the demand connection point [11]. The overvoltage-instability literature itself now records the observable: the 2026 review

D. J. Hume is with the Electricity Authority, Wellington, New Zealand (e-mail: corresponding author details on submission). ORCID iD: https://orcid.org/0009-0006-6920-0598.

This is descriptive analysis of public regulatory metering and information-disclosure data. The views expressed are the author's. No external funding was received. The analysis informs, but does not advocate, a live reactive-power pricing policy question (Section VI-D).

A reproducibility package (the analysis notebooks that compute every number and figure in this paper from public data) accompanies the work.

This is the *extended version*, including the complete measurement-error analysis (Appendix A), the mains-filter appendix, and supporting exhibits; a short version accompanies it in the same record.

of overvoltage instability mechanisms notes, among its causes of voltage rise, that cable substitution has "change[d] the power factor to leading in several urban substations" [12]—an observation offered without citation, and attributed wholly to the network's cables rather than to any change in what the connected demand draws. Every system in this literature runs 230-volt mains; Section V-B returns to that regularity.

B. Prior measurement and decomposition

The closest measured system-level series is the British one [1], [2], which characterises roughly eight years (about 2005–2013) of reactive demand at grid supply points and projects the trend forward from load-composition modelling and scenario projection; it supplies neither a multi-decade measured record nor a quantified demand-versus-network share of the realised drift. At the transmission–distribution interface, Javed *et al.* [13] characterise the consequences of capacitive reactive export in a Netherlands network, Baghban-Novin *et al.* [14] simulate feeder undergrounding and distributed generation on a Danish test system, and a Slovak study [5] links growing capacitive flow into the transmission network to the changing nature of the distribution network; none is a long measured record and none attributes a quantified demand-versus-network share.

The single study closest to the present decomposition is Bosisio *et al.* [15] on the Milan distribution network. Using measured 15-minute active and reactive power at 37 high-voltage/medium-voltage transformers, it names the same three-term balance at the distribution–transmission boundary used here—the reactive power withdrawn or injected by customers, that consumed by the cables' inductance, and that produced by the cables' capacitance—and in the indexed English-language literature it is, to our knowledge, the only prior study to articulate this split explicitly on measured boundary data. It differs from the present work on three points that matter: it compares two years (2019 against 2020, across a COVID-19 demand shock) rather than a multi-decade drift; it assigns no numerical share to the three terms; and where it attributes dominance it concludes that the leading flow follows from the capacitive nature of the Milan cables, with reduced demand amplifying rather than causing it—on which term dominates, its reading runs opposite to ours. We treat it as complementary: it confirms the framework on measured data for one heavily cabled city, its cable-dominant reading for that network is consistent with our own cohort result that cable intensity shapes where net-leading territory is reached first (Section IV-A), and it leaves open the national, multi-decade, quantified attribution.

C. The realised risk

In 2025 two power systems suffered major blackouts whose official investigations found a leading-reactive/overvoltage mechanism at their core: the Final Reports of the European Network of Transmission System Operators for Electricity (ENTSO-E), both published 2026, on the Iberian Peninsula event of 28 April 2025 [16] and on the North Macedonia event of 18 May 2025 [17], detailed in Section VI-C. What matters here is what those investigations could not do. Both reports treat the capacitive surplus as a network-side quantity and low demand as a magnitude rather than as a fleet whose reactive character has itself changed; neither distinguishes nor quantifies a demand-side composition shift from network charging. The Iberian expert panel models the reactive response of load to voltage, but its load model's reactive voltage exponents come from a table of typical values by load class—how the reactive power of demand varies with voltage, not what it was—and the North Macedonian report carries no load power-factor assumption at all; on two independent full-text reads of each report, neither states the aggregate reactive character of demand anywhere. The Iberian panel names the gap itself: modelling the transmission–distribution interfaces accurately, it notes, would need "information on load composition" [16]. These are not criticisms of investigations that reasoned from the data available to them; they identify the space a long measured record can fill. The field's current synthesis has the same shape: the 2026 mechanisms review [12] gives as its causes of voltage rise corridors below surge-impedance loading, cable substitution, synchronous-generator decommissioning, and fixed-power-factor converter operation—network and generation throughout—representing load as lagging or unity power factor in every model, citing no measurement of demand reactive character, and calling for none.

Operational practice has the same shape. Australia's transmission connection point forecasting methodology computes power factor at the transmission–distribution boundary from measured active and reactive power, and labels each point leading or lagging; but it takes that reading from the top 1% of half-hours ranked by active power, and holds the power factor constant over the forecast horizon [18]. Where it does anticipate the light-load power factor changing, it attributes the change to inverter standards. The measurement is made, at the peak.

D. Contribution

This paper makes a layered contribution.

Contribution 1 (measured trajectory). Using regulatory half-hourly active and reactive power at New Zealand grid exit points, we measure the system's reactive character at supply-point resolution over 29 years (1997–2025) on a balanced panel—the same grid exit points in every year, so sites entering or leaving the record cannot manufacture the trend—characterise its rate and crossing, and show the trajectory is a measured phenomenon and not a metering artefact. The computation reuses settlement metering that any operator holds, so the same measurement is available to any system.

Contribution 2 (decomposition of the drift). We decompose the drift into a demand-side load-composition component and a distribution network cable-charging component. The magnitude is carried by a first-principles charging calculation that computes each network's cable charging directly from its disclosed circuit kilometres (Section II-D) and so fits no cable coefficient; evaluated over the 2013–2025 disclosure window, it puts the demand-side (*organic*) share of the drift at about 80% (physical band 75–88%), with two statistical methods corroborating the direction over the full 29-year record but not themselves pinning the share. We report a measured direction and dominance and do not claim a point-identified split.

Contribution 3 (the term identified). We then identify what the demand-side driver is physically doing. The deepening is load-independent—as large at the flat evening peak as overnight—so it behaves as a standing shunt element, permanently energised, not as a change in how the load draws reactive power while operating. And it lives behind the connections: across grid exit points the 2013–2025 deepening is proportional to the number of connections served, with no detectable connection-independent residual; refitted year by year, each connection's standing contribution sits slightly on the inductive side of zero at the start of the record, crosses zero early in the 2010s, and grows every year thereafter—about 210 VAr per connection added over 2013–2025, read off the level history and reproduced within 10% by the fitted endpoint change—and it accumulated faster over the second half of that window than the first (Section V). The load fleet's own standing shunt term is moving capacitive, not merely drawing fewer lagging vars. We advance the mandated electromagnetic-compatibility filter capacitance as its candidate device layer (a labelled hypothesis), identify the decisive low-voltage measurement that would settle it, and note that both of the scaling test's inputs—settlement metering and connection counts—are records any operator holds.

The significance is what the reversal does to analysis: the direction of the binding voltage-security question reverses; the automatic last-resort defences and the margin tooling of the undervoltage era do not transfer; and the constant-lagging-power-factor load archetypes of planning and protection studies no longer describe the light-load fleet (Section VII)—a qualitative synthesis, not a defence-scheme or load-model redesign, which remain outside the paper's scope. Section III measures the trajectory; Section IV attributes it between fleet and network; Section V identifies the term and tests its scaling; Sections VI and VII set out the overvoltage consequences and the analysis implications; Section VIII collects future work.

This work extends the author's EEA 2025 conference paper [19], which described the 2009–2024 aggregate trend qualitatively. The present paper adds twelve further years of baseline back to 1997, in the firmly lagging regime; grid-exit-point spatial resolution; a quantified rate and crossing with an explicit artefact test; the decomposition of the drift; the connection-scaling identification; and the two post-EEA ENTSO-E Final Reports as an independent evidentiary anchor. Consistent with its descriptive scope, the paper reports the measured trajectory and the decomposition and notes that they inform a live reactive-power pricing question, without making any policy recommendation.

II. Data and Method

A. Sign convention and primary variable

Reactive power carries a direction that is the entire point of this study. We use the convention $Q < 0$ for *leading* (capacitive, voltage-raising) and $Q > 0$ for *lagging* (inductive, voltage-lowering). We lead throughout with the signed reactive power in MVAr, which is additive across supply points and has no discontinuity at unity, and present power factor only as a familiar comparator. Power factor is non-additive, so where a system power factor is quoted we sum P and Q across the panel first and derive $\mathrm{PF} = \Sigma P/\sqrt{(\Sigma P)^2 + (\Sigma Q)^2}$ rather than averaging power factors.

B. The grid-metering record and the balanced panel

The primary data is half-hourly real and reactive power at every grid exit point (GXP), the substations where the national transmission grid hands electricity to the local distribution networks, from 1997 to 2025, published by the New Zealand Electricity Authority on its Electricity Market Information (EMI) platform. Each per-year file is half-hourly for the whole year, indexed by trading date and trading period (48 half-hour periods per day), with a real-power and a reactive-power column for each GXP. Over the record, 238 distinct GXPs appear; a balanced core of 132 is present in all 29 years.

The series exists because a rule required it. The Electricity Governance Rules obliged the Electricity Commission to establish and maintain a centralised data set to support planning [20], and the half-hourly record assembled for it in 2004 was drawn from the settlement metering of the market's own start, running back to 1 October 1996—the old metering files of the Electricity Corporation of New Zealand, the state enterprise that once owned both generation and the grid, and the MV90 and Avalon systems that succeeded them [21]. Its stated reason for inclusion was demand forecasting and the Grid Investment Test: active-power problems. Reactive power entered that specification only as a plant parameter—generator reactive ranges, station voltage control, capacitor bank kVAr. The reactive column at the boundary has therefore been recorded for twenty-nine years because settlement metering records it, not because it was the object of anyone's question.

We reduce each GXP's year to a small set of features, of which the headline quantities are the average overnight and evening-peak reactive and real power. Following the prior EEA analysis, the overnight window is trading periods 6–10 (approximately 02:30–05:00, the deepest part of the night and the lowest demand) and the evening peak is trading periods 36–38 (approximately 17:30–19:00). We also record, for each GXP-year, the fraction of overnight half-hours that were leading. The full feature table is 5,261 GXP-year rows, one per GXP per year.

The single largest way a 29-year trend could be spurious is a change in the set of measured GXPs over time: new urban, cable-heavy sites appearing and old rural ones dropping out would manufacture a leading trend from bookkeeping alone. The primary defence is the *balanced panel*: only the 132 GXPs present in every one of the 29 years, so any change is a change in the same sites rather than a change in which sites are measured. We call that turnover—grid exit points entering and leaving the measured set—*churn*; the balanced panel is churn-controlled by construction ("balanced" in the panel-data sense, the same sites in every year, not the three-phase sense). We follow one rule throughout: *trends on the balanced panel, snapshots on the full panel*. The paper's subject is the

TABLE I
THE NATIONAL OVERNIGHT TOTALS, AND THE SAMPLE EACH COMES FROM

Sample	Window	Overnight reactive power
Balanced demand panel, 123 GXPs *(the headline)*	1997–2025	$+466 \rightarrow -451$ MVAr
Balanced full panel, 132 GXPs	1997–2025	$+673 \rightarrow -296$ MVAr
Clean and clean-strict cohorts, 119 and 92 GXPs	1997–2025	about -300 MVAr in 2025
Charging footprint, 29 networks	2013–2025	-541 MVAr in 2025, drifting -49.9 MVAr/yr
Connection-scaling panel, 114 GXPs	2013–2025	$+188 \rightarrow -182$ MVAr (medians)

distribution networks; restricting the balanced panel to demand networks (excluding a handful of generator, industrial, and rail connection points) leaves 123 GXPs. We report both the 132-point and 123-point figures and keep them labelled; they are the same trend at the same rate (Section III). The residual churn bias is signed: the demand grid exit points excluded from the balanced panel (post-1997 entrants and exits) are by 2025 on average *more* leading than the panel (median -0.28 against -0.18 MVAr/MW) and drift faster (-0.020 against -0.018 MVAr/MW/yr), so the balanced panel, if anything, understates the national drift. Five national totals follow, each on the sample its method requires, and Table I sets them side by side. They differ by sample, window and summary statistic rather than by measurement; a reader wanting one figure for New Zealand should take the first row.

C. Metering provenance and accuracy

The active and reactive power at each grid exit point is settlement-grade revenue metering owned by the national grid owner and system operator (Transpower), the registered metering equipment provider for these points. Grid metering is the highest-accuracy category of the regulatory Metering Code [22], certified by an approved test house and periodically re-certified and inspected. The present fleet is Schneider PowerLogic ION8800A meters, Class 0.2S for active energy under IEC 62053-22 [23], four-quadrant (import and export active and reactive), with Class A power-quality measurement under IEC 61000-4-30 [24], installed across roughly 150 grid sites in 2010–2013 [25], replacing legacy PSI Quad4 meters dating from about 1994 [26]; the reactive series thus rests on four-quadrant revenue metering for the modern record and on the older, coarser Quad4 instrumentation for the early record.

At a grid exit point the active-energy channel is held to Class 0.2 while the reactive channel is held to the looser Class 2–3 (about ± 2–3.5%) of IEC 62053-23 [27], with reactive accuracy specified only above 20% of rated current; as a share of the reading, reactive measurement is least accurate at light load and near-unity power factor, where the reactive component is small while current-transformer phase-angle error is largest. This asymmetry is the international norm, because active energy is the settled quantity. The reactive energy of the metering standards is the fundamental-frequency (*displacement*) quantity of IEEE Std 1459 [28]: the reactive power set by the phase angle between the voltage and the 50-Hz component of the current. The harmonic currents drawn by power-electronic loads add apparent power (distortion power) but accumulate no reactive energy on the meter, so the trend measured here is in fundamental-frequency reactive power—the component that drives the voltage rise of Section VI—with harmonic distortion out of scope. The cited standard does not by itself settle which quantity a given meter records, and the standards are moving on the point: the classes of IEC 62053-23 are being withdrawn into IEC 62053-24. The record supplies the check the standard does not. A distortion component would scale with the load operating, and so would concentrate in the loaded evening window—where Section V-A measures the deepening as near-equal in both, the same structure that bounds the $P \sin \beta$ term.

Neither the accuracy classes nor the one metering transition in the record can account for the measured drift; Appendix A carries the arguments in full. Class-bounded *random* error is bidirectional, averages down under aggregation, and cannot manufacture a near-monotonic 900-MVAr swing through zero; the one error that does *not* average down (a systematic current-transformer phase-angle bias of the form $P \sin \beta$, concentrated in exactly the light-load window this paper measures) is bounded in Appendix A to a near-static offset some fifty times smaller than the swing, contributing about 0.1 MVAr/yr of apparent drift; the staggered 2010–2013 fleet replacement is anchored out by the record's endpoints, with the modern-era drift, if anything, steeper; and a test for a synchronous system-wide re-base finds none. We therefore treat the multi-decade *drift* as robust while regarding the standing reactive *level* on any single night as carrying more measurement uncertainty, consistent with the level being the weaker claim of Section IV.

D. The asset (parameter) record

To describe each network's physical make-up we assemble a per-company, per-year table from the Commerce Commission's regulated information disclosures: circuit length split into overhead and underground kilometres at each operating voltage (Schedule 9c, disclosed consistently from 2013), capacitor-bank counts (Schedule 9a), demand and connection counts and embedded generation (Schedule 9e), and the regulated asset base (Schedule 4). The disclosures are mapped to the EMI network codes through a 29-year validated correspondence, time-aware because ownership itself changed under the record: 34 demand grid exit points (32 of them in the balanced panel) changed network code, almost all from the breakup of UnitedNetworks and the onward sale of its Wellington network (successor codes appear 2003–2013), plus one Nelson-region boundary change. The metering panel is attributed per year from the metering files themselves, so the trajectory follows every change; the cable-dose analyses of Section IV are run under both a per-year and a physical-continuity (successor-network) attribution, with the sensitivity reported there. Two data-quality choices are made explicitly: we retain only the "All"-network roll-up rows so that multi-network companies are not double counted, and we flag a 2014–2015 definitional break in the capacitor counts (a widening of reporting scope, not new plant) so that a paperwork change is never read as a physical one. The capacitor series is counts only, with no MVAr ratings or installation dates, and begins in 2013; we use it as a direction-only proxy—a stand-in that can indicate direction, not size.

E. Confounds in the metered reactive power

A grid exit point meter records the *net* reactive power at the boundary, which is not in general a clean distribution offtake:

$$Q_{\text{metered}} = \underbrace{Q_{\text{load}} + Q_{\text{cable}}}_{\text{the subject of this paper}} - Q_{\text{embedded gen}} \pm Q_{\text{TP plant}},$$

where the last two terms are *confounds*: signals mixed into the same metered reading that are not the subject of this paper. An embedded *synchronous* generator (hydro, geothermal, or cogeneration) regulates voltage and sets its reactive output by the voltage it sees rather than by local load; and at some substations a Transpower voltage-regulating device (a static var compensator or static synchronous compensator (STATCOM), a synchronous condenser, or a switched capacitor or reactor bank) shares the substation with the offtake, with the revenue-metering boundary determining whether it registers in the metered flow. One behavioural diagnostic catches all of these, whichever party owns the plant—a network's own large regulating compensation would be flagged identically: a clean distribution offtake's reactive power tracks its load, so a straight-line fit predicting Q from P explains an appreciable share of its variation ($R^2 \approx 0.3$–0.5), whereas voltage-regulated reactive is decoupled from load ($R^2 \to 0$, with a large residual the load does not explain). Computed on three spread-out years (2016, 2019, 2022) so that a flag reflects a stable trait, the screen isolates six *decoupled* grid exit points—*contaminated*, in the sense that the metered reactive power includes plant that is not the distribution offtake, whether embedded generation or transmission-owned voltage-regulating plant: ISL0661 and BRY0661 (Islington and Bromley, Christchurch: substations hosting Transpower voltage-regulating plant—static var compensators, switched capacitor banks, and shunt reactors—and serving a distribution network extensively reconfigured after the 2010–11 earthquakes), PEN1101 and HOB1101 (Auckland), BPE0331 (Bunnythorpe), and TWH0331 (Tuai, with the Waikaremoana hydro stations).

This matters overnight specifically: the overnight minimum removes generation that merely stops, but not plant that regulates voltage around the clock. That includes the synchronous fleet—hydro, geothermal and cogeneration regulate voltage whatever the hour—and, increasingly, inverter-based plant running a night-time reactive mode, which holds a voltage setpoint at zero active power and so is not removed by darkness either. The diagnostic above is behavioural rather than technology-specific, so it catches both. One illustrative public case is the Cobb hydro station, divested by Transpower to Network Tasman around 2011: its pricing node was retired and its output now nets into the Stoke grid exit point (STK0661), a "lost node" whose metered reactive no longer represents a clean offtake. We flag these sites rather than discard them silently, and we show in Sections III-B and IV that the trajectory and the decomposition are robust to their removal: the contamination affects the absolute *level*, not the direction, intensity, or attribution of the drift.

F. Analysis methods

The trajectory is summarised by ordinary linear slopes for headline rates and, for robustness, by Theil–Sen slopes [29]: the median of the slopes through every pair of years (406 pairs for a 29-year series), an estimator that a few anomalous years cannot move, standard in long-record environmental trend monitoring, used here on both the national and per-GXP series; where the two estimators agree—as they do throughout—a trend rests on no small set of years. The test that the trend is not a metering artefact (Section III-B and Appendix A) removes each GXP's own Theil–Sen trend and looks in what remains for a step shared across sites in the same year, using a change-point detector and a coherence statistic. The decomposition (Section IV) uses three methods: a clean-cohort comparison and a mixed-model cable dose-response with a company-cluster bootstrap (validated on synthetic data before use), which share a common underground-cable proxy and so are not independent of one another; and a first-principles cable-charging calculation, $Q = \omega C V^2 \ell$, with a $\pm 35\%$ physical band on cable capacitance carried through to the result, which fits no cable coefficient and is independent of the other two. All analysis is reproduced from public data in the accompanying notebooks.

III. The 29-Year Reactive Trajectory

A. Lagging to leading, overnight

Fig. 1 shows the central empirical result. Summed across the balanced demand panel, mean overnight reactive power fell from $+466$ MVAr (lagging) in 1997 to -451 MVAr (leading) in 2025, a near-monotonic linear drift of -31.1 MVAr/yr (robust Theil–Sen slope -31.3 MVAr/yr, 95% confidence interval (CI) $[-34.0, -28.1]$, the rank-based interval taken as order statistics of the sorted pairwise slopes [29], which like the estimator itself treats the annual values as serially independent; since consecutive years are in fact strongly correlated, read it as the spread among the pairwise slopes rather than a coverage guarantee), crossing into net-leading overnight in 2016. On the wider 132-point balanced panel that also includes non-distribution connection points, the same drift is $+673 \to -296$ MVAr at -30.3 MVAr/yr, crossing in 2020; the rate is essentially identical and the leading endpoint is, if anything, stronger on the demand-only panel once lagging industrial load is removed. The two panels are the same trend, labelled distinctly and never blended into one figure. Expressed per megawatt of overnight load, the drift is about -0.018 MVAr/MW/yr; we lead with this intensity and with the share of networks gone leading because, unlike the absolute MVAr total, they are insensitive to a few large contaminated nodes (Section III-B). The denominator is not doing the work: overnight load on the panel grew from about 1,680 MW in 1997 to about 1,960 MW in 2025. In the familiar comparator of Section II-A, the overnight aggregate power factor moved from 0.964 lagging to 0.975 leading—a numerically small excursion either side of unity concealing a 900-MVAr reversal, which is why the signed reactive power is the working variable throughout.

The diurnal contrast is itself a result. The evening peak crossed net-leading only in 2022 and remains far less leading than overnight, which locates the net-leading regime firmly at low load. Expressed as a fraction rather than a sum, the mean share of overnight half-hours that are leading rose from about 1% in 1997 to about 74% in 2025: overnight leading became routine rather than exceptional.

B. Measured, not an artefact; robust to contaminated sites

Two features of the record answer the metering-artefact objection directly, and a further test closes the one gap they leave.

First, the drift does not rest on the older, less homogeneous early data. The metering and data pipeline modernised across the record (notably the move to the present Electricity Market Information system), and the one visibly suspect feature is an early step in the overnight leading fraction between 2000 and 2001, consistent with a change in metering vintage. Restricting to the homogeneous modern era removes any such concern, and the drift is if anything slightly steeper: -33.0 MVAr/yr over 2002–2025 against -31.1 MVAr/yr over the full record. A trend manufactured by early-era inhomogeneity would fade on the clean modern data, not strengthen.

Second, a measurement artefact cannot reproduce the trend's physical structure. The net-leading crossing is specific to the overnight window—the evening peak stays lagging for years longer (Fig. 1)—while the deepening beneath the crossings is near-equal in the two windows over 2013–2025, with evening-peak load essentially flat (Section V-A): the signature of a standing capacitive term netted against different amounts of lagging load. The one systematic metering bias that does not average down scales with the metered load ($P \sin \beta$, bounded in Appendix A) and would deepen the heavily loaded evening window far more than the lightly loaded overnight one, which is not observed. Nor is the shift seasonal: recomputed separately for winter (June–August) and summer (December–February) months, the overnight aggregate drifts at -31.1 and -30.8 MVAr/yr respectively, so the trend is not an artefact of heating-season load composition. The drift also tracks each network's underground-cable intensity (Section IV); a metering error has no reason to correlate with cable kilometres. Nor does a metering artefact at the grid exit point have a mechanism that scales with the customers behind it: the 2013–2025 deepening grows linearly with each grid exit point's connection count, and that connection-scaling term carries the large majority of it (Section V-C). This combination of a diurnally structured, cable-correlated, connection-scaling shift is one that a change in measurement convention cannot counterfeit. The charging calculation of Section IV is not a further witness here: it *partitions* the measured drift rather than reproducing it, so an instrument error would sit inside the residual it assigns to the fleet.

These two arguments address a gradual or staggered change, such as piecemeal meter replacement across sites. A single system-wide re-base—a one-date change of sign convention or central processing that would step every supply point at once—is different; we test for exactly that in Appendix A and find no such event. The lagging-to-leading drift is therefore a measured property of the system, not an artefact of how it was metered.

A second objection, distinct from a metering artefact, is that the trend could be carried by a few grid exit points whose meters do not see a clean distribution offtake (Section II-E). We test it directly by removing them. Dropping the six *decoupled* grid exit points whose reactive power is set by plant or embedded generation (the *clean* cohort), and more strictly also the steady-generation and net-export points (the *clean-strict* cohort), we re-measure the trajectory on the balanced demand panel (Fig. 2).

Two quantities behave very differently, and the difference is the point. The absolute total and the MVAr/yr slope *shrink* when the contaminated sites are removed—the 2025 total from -451 to about -300 MVAr and the slope from -31.1 to -23.4 MVAr/yr—because two of the removed nodes (Islington and Bromley) carry large, load-decoupled leading values, so the absolute *level* is partly inflated by contamination. The per-MW drift intensity, by contrast, is essentially unchanged (-0.0175, -0.0178, and -0.0180 MVAr/MW/yr across the full, clean, and clean-strict cohorts), and the share of networks net-leading overnight by 2025 is likewise stable (75%, 74%, 80%). The quantities that describe the phenomenon—its intensity per unit load and its near-universal reach—do not depend on the contaminated nodes; only the headline *size* does. This is why we lead with the per-MW drift and the share-leading migration and treat the absolute spine as a contamination-sensitive companion.

IV. Decomposition: Demand vs Network

The policy-relevant question is how much of the drift is the network's own cables, which inject leading reactive power as a distributed capacitance, and how much is the changing make-up of electricity demand itself: the retreat of inductive plant (simple motors) and the accumulation of power-electronic equipment (LED lighting, switch-mode supplies, heat pumps and other variable-speed drives). We call the second part *organic*: it is in the load fleet, not the wires. If the drift were mostly cables it would be a familiar network-planning problem; if it is mostly the demand fleet it is structural, nationwide, and outside any single network's control. We approach the question three ways; the two statistical methods share a common underground-cable proxy, while the physics-based method fits no cable coefficient and is independent of both. What the demand-side component physically *is*—the question the decomposition leaves open—is taken up in Section V.

A. Method 1: a clean-cohort contrast

History handed us networks at opposite ends of the cable spectrum. Some distribution businesses are almost entirely

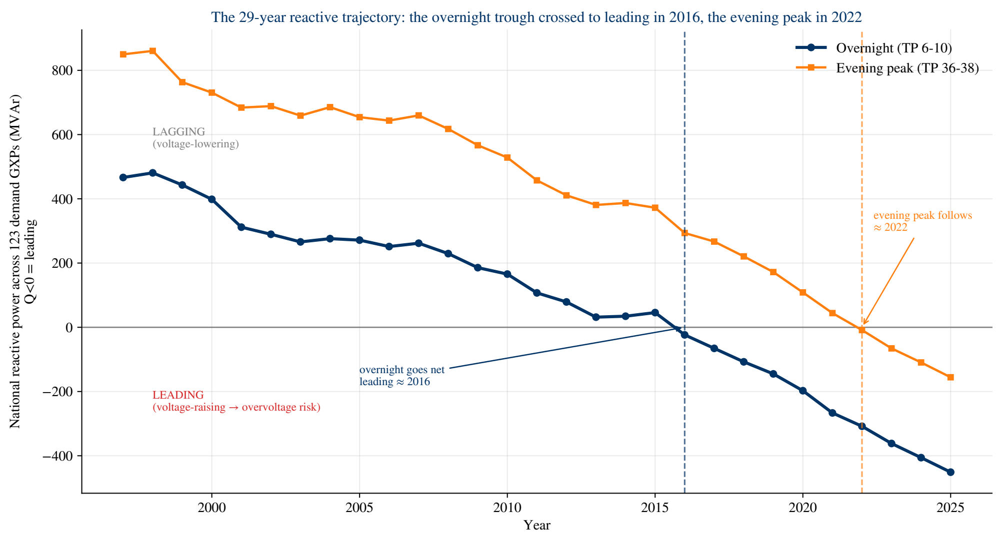

Fig. 1. The 29-year reactive trajectory on the balanced demand panel (123 grid exit points present in all years). Overnight (trading periods 6–10) drifts from strongly lagging ($Q > 0$, voltage-lowering) to clearly leading ($Q < 0$, voltage-raising), crossing net-leading in 2016; the evening peak (trading periods 36–38) follows much later. The diurnal split (the problem lives overnight at low load, not at the busy evening peak) is the signature of a standing capacitive term dominating when load is least able to mask it; Section IV attributes that term mainly to the demand fleet rather than to network charging. Sign convention: $Q < 0$ is leading.

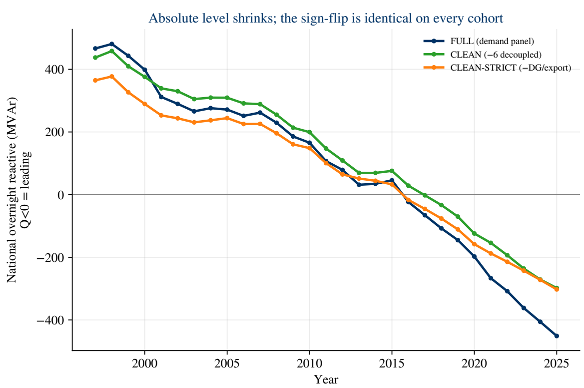

Fig. 2. The trajectory is robust to removing contaminated grid exit points: the national overnight total on the full demand panel and on the clean and clean-strict cohorts (the latter also removing distributed-generation, "DG", and net-export sites). The absolute level falls as large decoupled nodes are removed, but every cohort makes the same lagging-to-leading crossing, and the per-MW drift intensity is unchanged across cohorts (-0.0175, -0.0178, -0.0180 MVAr/MW/yr). The contamination inflates the level, not the direction or intensity of the drift.

overhead line and have almost no underground cable; overhead line injects little leading reactive power, so these networks have almost no cable contribution. If their overnight reactive power still drifts leading, that drift can only be the demand fleet. We compare reactive power per MW of load (so network size cancels), load-weighted within each cohort (larger sites count proportionally more), for networks at or below 12% underground (*clean* in this method's sense: almost cable-free, distinct from the decontaminated cohorts of Section III-B) against networks at or above 40% underground (cable-rich), shown in Fig. 3(A).

The clean cohort drifts from $+0.373$ to $+0.065$ MVAr/MW (slope -0.0101/yr), ending near balanced; the cable-rich cohort drifts from $+0.205$ to -0.306 MVAr/MW (slope -0.0134/yr), crossing well into leading. The ratio of slopes ($0.0101/0.0134 \approx 0.75$) puts the demand-side share of the cable-rich cohort's drift at about 75%, cable the remaining 25%. The reading rests on two assumptions the split depends on, stated plainly: that the organic per-MW drift is common across the cohorts (to the extent urban load fleets modernise faster than rural ones, the cable share is overstated), and that the at-most-12%-underground cohort carries no material cable term (to the extent it does, the demand share is overstated); the two possible violations pull the split in opposite directions.

Three further caveats bound the ratio. Schedule 9c offers two circuit-length tables that differ by a few points of %UG (percentage underground) for cabled networks, and Method 1 gives about 75% under the "total length for supply" table against about 69% under the "by operating voltage" table (Unison sits on the 40%-underground boundary at 39–45% across averaging choices, so its cohort membership, though not the load-weighted ratio, turns on the same choice). A separate circuit-length series taken over all grid exit points rather than the balanced panel yields a wider, roughly 90/10 reading. And the ratio moves with how the grid exit points that changed network (Section II-D) are attributed: carrying each site's successor cable dose throughout (the wires being physically continuous), rather than entering it in the cable-rich cohort only once its successor company discloses, steepens the cable-rich drift to -0.0159/yr and moves the split to about 64% demand; the clean cohort contains no such site and is identical under every attribution, so the organic direction is untouched.

The *direction* is therefore robust while the *exact ratio* is not, which is why we treat Method 1's ratio as a hypothesis and bring two further methods. The contrast is also robust to the

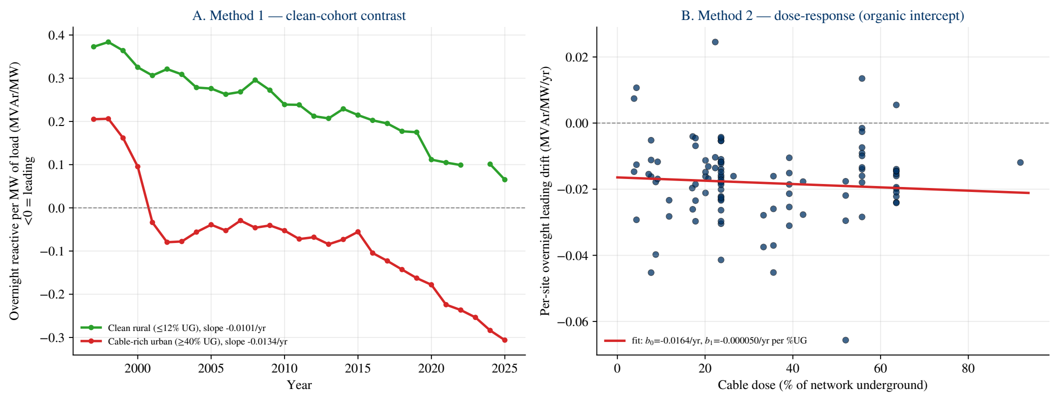

Fig. 3. The two statistical methods. (A) Method 1, the clean-cohort contrast: even clean rural networks (at most 12% underground, so almost no cable charging) drift leading per MW of load, isolating the demand-side component; cable-rich urban networks (at least 40% underground) drift slightly faster and cross further into leading. The slope ratio implies roughly 75% of the cable-rich cohort's drift is demand-side (64–90% across attribution, cable-intensity, and panel definitions; Table III). (B) Method 2, the validated dose-response: each point is a GXP's overnight leading drift against its cable dose (its network's percentage underground). The drift is already strongly leading at zero cable (the fitted intercept b_0, the organic demand-side signal); the slope with cable is weakly identified (its interval crosses zero), so the exact organic share is not pinned by statistics alone.

metering contamination of Section II-E: the cable-rich cohort contains the two decoupled Christchurch nodes (Islington and Bromley), and removing them softens the cable-rich drift to -0.0129/yr and moves the split to about 78% demand, 22% cable—so the contamination, if anything, overstated the cable share, and removing them strengthens the demand reading. And although cable is the minority of the drift, it is the marginal factor that tips a network from balanced into net-leading: the clean cohort ends near balanced while the cable-rich crosses into leading, so cable intensity shapes *where* overvoltage appears first even though demand composition drives the trend.

B. Method 2: a validated dose-response

The second method asks whether the networks with more cable drift faster. Each GXP is reduced to one number—the Theil–Sen slope of its overnight reactive power through the 29 years, scaled by its own typical size—and those per-site drifts are then fitted against the site's *cable dose*, the percentage of its network that runs underground. The line has two coefficients, and only one of them is this paper's result. At zero cable there is no cable charging, so any drift remaining at that end of the line must come from the demand: the intercept b_0 is the organic drift. The slope b_1 is the extra drift per added point of underground—the cable contribution.

Two features of the fit follow from how the dose is recorded. Cable dose is a property of the *company*, so every site in a network carries the identical value and the sites are not independent. The model therefore lets each company sit at its own baseline (a random intercept per company), and the uncertainty comes from a *cluster bootstrap*: the fit is re-estimated on thousands of datasets drawn at random, with replacement, from the data itself, and the reported interval is the spread of those answers—drawing whole companies rather than single sites, so that the dependence is carried into the interval. The interval is computed by refitting within each company-resample by ordinary least squares; refitting the mixed model instead leaves it unchanged at the reported precision.

Before any use on the real data, the estimator was validated on synthetic panels with known planted answers, built on the real company structure and real cable doses and run through the identical machinery in two scenarios (a planted cable effect, and none); the full protocol and results are in the accompanying notebooks. The validation licenses a specific and limited claim. The estimator recovers the sign and magnitude of the organic drift reliably in both regimes. It point-identifies (pins to a single number) the organic *share* only when the cable effect is itself identified, and the reason is arithmetic: that share is $b_0/(b_0 + b_1 d)$ at dose d, which puts b_1 in the denominator. A precise numerator over an uncertain denominator is an uncertain ratio, so on the real data the share cannot be pinned even though b_0 is, and we rest no magnitude on this method. Line-fitting can neither manufacture a split here nor, with a cable effect indistinguishable from zero, pin one; the magnitude falls to Method 3.

On the real data (Fig. 3(B)), the organic drift is $b_0 = -0.016$/yr (95% CI $[-0.021, -0.010]$), leading in 100% of bootstrap resamples: unambiguous and dominant. The cable slope is $b_1 = -0.00005$/yr (95% CI $[-0.00037, +0.00012]$), which crosses zero—weakly identified, because cable dose is a company-level trait with only about 23 distinct values—so we deliberately publish no tight interval on the share (read across the cable range, the point estimate runs from 93% at the median dose to 78% at the most cabled networks, consistent with 100%; the point estimate is the single best-guess number before any range is put around it). Three robustness checks hold: adding capacitor intensity to the fit as a control (the cable effect read at fixed capacitor intensity) moves b_0 by only about 10% and leaves it strongly leading (consistent with the static-to-declining capacitor fleet of Section VI-B); the low correlation between cable dose and distributed-generation intensity (-0.22) indicates the organic signal is not an artefact of where embedded generation sits; and restoring the four sites dropped for want of a disclosing owner in the Section II-D mapping under their successor's cable dose moves b_0 by under 1%.

A fourth check replaces the dose measure altogether: refitting with each network's computed charging intensity as the dose—Method 3's physical $\omega CV^2\ell$ (Section IV-C) summed and taken per MW of maximum demand—moves b_0 only from -0.0164 to -0.0178/yr, with the cable term still crossing zero. The two dose measures are in fact *negatively* correlated across networks ($r = -0.23$): the near-all-overhead rural networks carry far more circuit length per MW of demand (69–89 km per MW at the overhead extreme against 9–11 at the most-cabled) and end up with *more* computed charging per MW than the most-cabled urban networks, so percentage underground is in part an urban-density measure rather than a charging-intensity one. That two nearly opposite dose definitions return the same organic conclusion is a stronger robustness statement than either alone. (The charging-intensity dose shares its per-MW denominator with the per-site drifts, which can bias the cable slope but not the zero-cable intercept; no reading here rests on the slope under either dose.)

Method 1's urbanisation confound applies here too, and in the same direction: the cable dose is a company-level trait, so if urban fleets modernise faster than rural ones some of that difference loads onto b_1 rather than b_0, overstating cable and understating the organic term. The bias is conservative for the reading we take.

C. Method 3: first-principles charging physics

The third method computes the network contribution directly from physics, with no fitted coefficient, so it sidesteps the weak-identification problem entirely. Any energised length of cable or line behaves as a distributed capacitance and injects a fixed leading reactive power $Q = \omega CV^2\ell$, where $\omega = 2\pi \cdot 50$ rad/s, C is capacitance per km, V the operating voltage, and ℓ the length. Underground cable has far more capacitance per km than overhead line. Using the published overhead and underground kilometres at each voltage from Schedule 9c, textbook per-km capacitances with an explicit $\pm 35\%$ band, and a band-by-band sum (charging scales with V^2, so high-voltage lines dominate), we compute the physical charging per network per year and subtract it from the measured overnight reactive power; the remainder is organic (Fig. 4).

The operating voltage in each band is its *nominal* value, held constant across the record, and since charging scales with V^2 a systematic drift in operating voltage would move the computed term and land the difference in the residual. Three things bound it. First, where the charging sits: 77% of the computed 2025 total is at or below 33 kV (Table II), on the distribution side of the grid exit point transformer, where the on-load tap changer holds voltage to a setpoint rather than letting it follow the transmission system—so most of the term sits behind a regulator, not adrift. Second, the direction of the documented adaptation: distributors facing rising light-load voltage have tapped *down* and re-tapped distribution transformers, which lowers the true charging below the computed value and makes the residual, and hence the organic share, *conservative*. Third, the size: re-running the whole decomposition under a per-year voltage ramp $k(t) = (1 + g(t - 2013))^2$ applied to the computed charging moves the central organic share by -7.8 percentage points for a 5% rise across the window and $+7.4$ for a 5% fall, and a sustained rise of 4.2% (0.35% a year for twelve years, against a statutory band of $\pm 6\%$ for most of the record) would be required to carry the share below the 75% floor of the physical band. The two mechanisms also pull against each other: a rise on the transmission side is what provokes the tapping down on the distribution side. The band is set to span published per-km capacitance values across common distribution cable constructions and cross-sections, and it is carried through to the result rather than quoted and dropped. The organic remainder is a residual, and we name the principal further terms it absorbs: transformer magnetising reactive power (lagging, so static or growing alike mask leading), series-reactance absorption (minimal at light load, and rising over the window with overnight demand rather than falling), and the distribution capacitor fleet (static-to-shrinking, Section VI-B, so its change also removes leading). Each is either second-order overnight or biases the residual toward lagging, so reading the residual as the demand-side drift is conservative in respect of these terms. It is not an exhaustive accounting: the Method 3 footprint carries no decoupled-node screen, so any embedded generation running a night-time reactive mode also sits in the residual. We therefore remove those sites rather than only naming them. Re-running the decomposition on the decontaminated footprint puts the organic share of the drift at 82% with the six decoupled nodes of Section II-E removed, and at 89% (physical band 86–93%) once every steady-generation and net-export site is removed as well. Charging is disclosed per network while the flags are per grid exit point, so each network's charging is scaled by its retained share of overnight demand; dropping whole networks instead leaves too few to read at the strict screen.

The direction is what this check delivers: every screen that removes embedded generation moves the share *up*, so the headline figure is not inflated by those sites and the conservative reading survives this term as well. *We do not restate the headline on this basis.* The decontaminated footprint is a smaller and different sample rather than a better measurement of the national quantity—those sites are real grid exit points carrying real reactive flow at the boundary—and the physical bands overlap, so the shift is not resolvable against the $\pm 35\%$ capacitance uncertainty that dominates this method. The check licenses reading $\sim$80% as conservative, not as understated.

Over 2013–2025 the measured overnight reactive power drifts at -49.9 MVAr/yr across all demand networks, of which the physical charging contributes only -9.2 MVAr/yr (cable length grows slowly) and the organic residual -40.7 MVAr/yr. The organic share of the *drift* is therefore about 80% (physical band 75–88%). Because this method fits no cable coefficient, it is independent of the two statistical methods; the division of labour is collected in Section IV-D. The window is set by the data: the disclosed circuit kilometres it runs on (Section II-D) are recorded consistently only from 2013, so the physics decomposes the 2013–2025 drift, about 45%

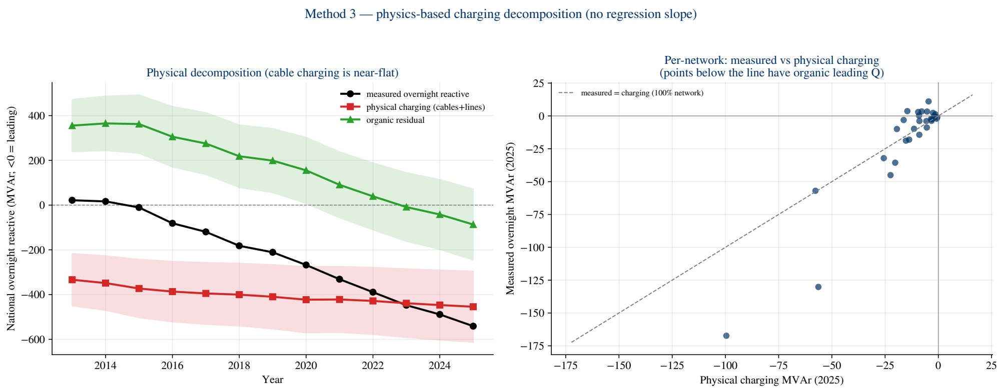

Fig. 4. Method 3, the physics-based decomposition over the all-network footprint (2013–2025, the years with consistent Commerce Commission circuit-length disclosures, from which the charging is computed). The physical cable and line charging (red, with the $\pm 35\%$ band shaded) is near-flat because cable length grows slowly, so almost all of the worsening trend in the measured overnight reactive power (black) is the organic residual (green). The drift is about 80% organic (physical band 75–88%). The right panel shows, per network, that most points lie below the unity line, i.e. carry organic leading reactive power beyond their charging.

TABLE II
COMPUTED PHYSICAL CHARGING BY VOLTAGE BAND, 2025 (CENTRAL CAPACITANCE VALUES, ON THE FOOTPRINT OF FIG. 4)

Band	**UG km**	**OH km**	**Share of charging**
6.6–11 kV	17,365	67,729	41%
33 kV	1,747	6,983	29%
50 & 66 kV	118	2,406	12%
>66 kV	52	537	11%
22 kV	795	3,488	6%
Low voltage (<1 kV)	31,884	23,552	0.2%
SWER	24	3,271	0.1%

of the record; extending the ∼80% share to the full 29 years is an inference, supported by the direction-consistent statistical methods (which do span the full record) and by the slow growth of cable length, not a second measurement. We stress that this all-network footprint rate (-49.9 MVAr/yr, 2013–2025) is a different dataset from the balanced panels of Section III (-31.1 MVAr/yr on the 123-GXP demand panel; -30.3 on the 132-GXP panel, 1997–2025) and from a separate cable-correlation analysis of the same public records, reported in the accompanying notebooks (≈ 46 MVAr/yr); these measure different things over different samples and are not interchangeable.

Table II breaks the computed charging out by voltage band, and it is why the band-by-band sum matters. Underground cable carries about 76% of the computed charging and overhead line the rest, with the total rising from 335 to 454 MVAr over 2013–2025 on this footprint. The low-voltage row is the instructive one: LV is by far the largest underground category—31,884 km, more than the 11 kV band's 17,365—and contributes 0.2% of the charging, because charging scales with V^2. A single-average-voltage treatment would misattribute it badly; the 6.6–11 kV and 33 kV bands, which carry most of the underground kilometres that matter, contribute about 70% between them.

A separate and more uncertain question is the composition of the leading reactive power *standing on the network today* (the level, as opposed to the drift). On the level the physics points the other way: a large, near-static cable and line charging baseline has always been present, and what changed is that the organic demand shifted from lagging—which used to mask the charging—toward leading, which no longer does. Today's net leading reactive power is then mostly long-standing charging *revealed* rather than newly created. The exact level split has a wide physical band and we do not quote a precise share for it; the level is a distinct, weaker claim and must not be confused with the drift result. We carry this only as the qualitative "uncovered charging" reading that informs Sections VI and VII.

D. Triangulation

Table III collects the three methods, which play different roles and are not all independent: Methods 1 and 2 both rest on the same underground-cable proxy, whereas Method 3 fits no cable coefficient at all. All three, though, consume the same Schedule 9c circuit-length disclosures—cohort definition and dose in Methods 1 and 2, the length ℓ in Method 3—so agreement among them cannot diagnose a systematic kilometre error, which would move all three coherently; under-counted cable would push every method toward the demand side.

The reading follows that division of labour. The *direction* is robust and identified: the organic drift is leading in 100% of bootstrap resamples while the cable contribution to the drift is not statistically distinguishable from zero, and together these imply the drift is dominantly demand-side. The *magnitude* is carried by the physics: the first-principles charging calculation, which fits no cable coefficient, puts the organic share at about 80% (physical band 75–88%). The two statistical methods are directionally consistent but, because the marginal cable effect (the extra drift per unit of cable) is not identified at the few company-level cable values available, do not themselves pin the share. We report the drift as dominantly organic and do not claim a point-identified split. Cable is the minority of the drift but the marginal factor in where net-leading territory is reached first.

TABLE III
THREE DECOMPOSITIONS OF THE DRIFT

Method	Establishes	Organic share of drift
1: clean-cohort contrast (cable proxy)	direction (shares the cable proxy with 2)	∼75% (78% with contaminated nodes removed; 64–90% across attribution, cable-intensity, and panel definitions)
2: dose-response (cable proxy)	direction / dominance	≥78%, consistent with 100% (cable term not pinned by the data)
3: charging physics (no fitted cable term)	**magnitude**	∼80% (physical band 75–88%)

A cross-sectional check agrees: ranking the demand grid exit points by how leading they now are, the most-leading group is not the most-cabled—the sites with the steepest drift and the highest leading fraction sit at roughly half the cable intensity of the most-cabled group, and the gap widens further when the decoupled Christchurch nodes of Section II-E are removed—so cable cannot be what drives the deepest-leading behaviour, independently confirming the demand-side reading (the full cross-sectional typology is in the reproducibility notebooks). The three methods share a subject—the *rate* at which the overnight reactive power moved—and none of them describes the standing level. Figure 4 separates the two, because the distinction carries the practical reading: the distribution network's charging is the larger part of the leading reactive power present tonight, and the demand is the larger part of why that total has moved.

V. The Demand-Side Term Identified: A Standing Shunt Term Behind Connections

The decomposition attributes the drift to the demand fleet; it does not say what in the fleet is doing it. Two measured properties narrow the answer, a specific physical candidate follows from them, and a scaling test probes the candidate's sharpest prediction.

A. Load-independent, around the clock

First, the drift is load-independent. Over the 2013–2025 window we summarise each grid exit point passing the full contamination screen (the clean-strict criteria of Section III-B, applied here to all sites metered in the window rather than to the 29-year balanced panel) by robust annual medians on wider windows than the Section II features (trading periods 1–12, midnight–06:00, and 35–39, 17:00–19:30). On the 114 such grid exit points with both endpoints metered, the median per-site change in reactive power is -2.25 MVAr overnight and -2.42 MVAr at the evening peak (median per-site ratio 1.06), while evening-peak load was essentially flat (median change $+2.9\%$). A change in how the connected load draws reactive power while operating would scale with the load operating—far larger at the peak than at 03:00—and so would the load-proportional metering bias bounded in Appendix A, whose spurious term goes as $P \sin \beta$. A near-equal deepening around the clock is instead the signature of a *standing shunt term*: always energised, indifferent to what the load is doing. It also reconciles the diurnal structure of Fig. 1: the two windows drift in parallel, and net-leading surfaces overnight first because the standing component is netted against more lagging load at the peak.

The peak/overnight comparison carries a second, quantitative reading that the load-independence argument does not need but which bounds it. A purely standing shunt term scales with V^2, and evening-peak voltage runs *below* overnight voltage, so such a term should deepen slightly less at the peak, not more. Taking equal deepening as the conservative null, the measured excess at the peak (-2.42 against -2.25 MVAr) is 0.17 MVAr, or about 7% of the peak change: an upper bound on the load-proportional component of the whole movement. Allowing the peak voltage to run 2–5% below the overnight value raises that bound to 11–16%. It is a bound and not an estimate—the load-proportional part could be zero—but it is a bound the record supplies for free.

The measured quantity is a net shunt term: What this test identifies is the *net* standing shunt term, and the distinction governs everything claimed after it. A standing shunt *inductance* has the same three signatures as a standing shunt *capacitance*: it is load-independent, it is permanently energised, and its injection scales with V^2. Writing the net as $Q_L - Q_C$, the record delivers $Q_L - Q_C$ in every year and never Q_L and Q_C separately, so a movement of the net is consistent with capacitance added, inductance removed, or any combination. Fig. 5B makes the point concrete: the per-connection term stands at $+41$ VAr (inductive) in 2009 and reaches -262 VAr by 2025, a movement of 303 VAr whose two limbs the measurement does not resolve.

Both limbs were moving inside the window, and the inductive one is not a second-order correction. The classes that count are those permanently energised at 03:00, which is a much narrower set than the fleet at large—anything switched off overnight contributes to the evening peak and not to the headline window, so residential lighting and its halogen transformers drop out of the inventory whatever their installed base. What survives that filter:

- *Linear transformer supplies.* A small mains-frequency transformer with a bridge rectifier draws its magnetising current whenever it is plugged in, and small cheap transformers magnetise poorly: no-load current of 20–40% of rated is typical, so a 6 VA unit stands at roughly 1–3 VAr inductive. Its switch-mode replacement, if it carries an X-capacitor at all, stands at up to a few VAr *capacitive*. The substitution swing is therefore 2–6 VAr per device rather than the 2–4 VAr the capacitance-only estimate of Section V-B credits—the estimate counts the capacitor added and not the inductance removed. Survivorship works the same way: the units that last longest are the ones nobody has a reason to touch, and those are disproportionately the permanently energised ones (doorbell and alarm supplies, gate and garage controllers, intercoms, low-voltage garden lighting), several of them wired rather than plugged and retired on the building cycle. The stock's inflow effectively stopped in the late

2000s, but the retirement rate of a stock with no inflow peaks a service life later, not when the inflow stops.

- *Magnetic-ballast lighting left on overnight.* Street lighting and commercial security, stairwell and display lighting run on wound ballasts at power factors near 0.5 lagging, are energised through exactly the measurement window, and converted to light-emitting diodes across the window.
- *Always-on motors.* Shaded-pole and split-phase compressors, extract fans, circulation and pool pumps, moving to inverter drives.
- *Distribution transformer magnetising reactive power.* Named in Section IV-C as a residual absorber, it belongs here too, because it has the same identification signature as the claimed device fleet: standing, connection-scaling, and inductive. A renewed fleet magnetises less.

A retirement moves the net exactly as an addition does, and neither the level nor the connection-scaling test can tell them apart. We therefore report the net term throughout and advance the device layer of Section V-B as a candidate for its *capacitive limb alone*, leaving the split as stated future work (Section VIII). Two routes to it are identified there: the standing power factor measured at the start of the record, which anchors the inductive limb at one endpoint, and the frequency sensitivity of the aggregate, which returns $Q_L + Q_C$ where the level returns $Q_L - Q_C$.

B. A physical candidate: the mandated EMC filter

Second, the term must live behind essentially every connection, because the drift's reach is near-universal across grid exit points (Section III-B). We therefore advance a specific physical candidate, labelled plainly as a hypothesis: the electromagnetic-compatibility (EMC) filter that practically every mains-connected electronic product is required to carry. A switched-mode device chops current at tens to hundreds of kilohertz, and conducted-emission limits (the international CISPR limits [30], covering roughly 150 kHz–30 MHz, a condition of sale in most jurisdictions, New Zealand included; the same obligation reaches household appliances through CISPR 14-1, on a lineage older still, and variable-speed drives through IEC 61800-3) oblige its manufacturer to stop that noise at the appliance's own terminals; the universal compliance solution is a passive filter directly across the mains input.

Its elements carry safety-class names [31] from where they connect: *X-capacitors* bridge line and neutral—the one position where a capacitor is permitted to be large (typically 0.1–2.2 μF), because a short circuit there is an overcurrent event the appliance's fuse clears rather than a shock hazard—while *Y-capacitors* run from the conductors to earth, where a short would electrify the chassis, so they must be built never to fail short and are held to nanofarads by touch-current limits; a common-mode choke completes the filter (Appendix B).

At 50 Hz the filter's only material injection is the X-capacitance, which sits across 230 V drawing pure leading current whenever the plug is live: 0.1–1 μF injects 1.7–16.6 VAr, around the clock, because the filter sits ahead of the rectifier and of any standby logic—it must, since the noise it suppresses would otherwise leak even in standby. At 230 V the arithmetic is $Q = \omega C V^2$: 0.1, 0.47, 1, and 2.2 μF inject 1.7, 7.8, 16.6, and 36.6 VAr respectively. The fleet is one worldwide design, so the capacitance is chosen once and the mains it lands on sets the draw: the same microfarad that injects 16.6 VAr here injects 5.4 VAr on North America's 120 V, 60 Hz mains and 3.1–3.8 VAr at Japan's 100 V—roughly three times the standing draw per device at 230 V as in North America, and four to five times Japan's. The Y-capacitors are not quite silent—where the appliance is earthed, the line-to-earth element injects too—but at nanofarad scale it is under a per cent of the X-capacitor beside it, and the numerous small always-connected devices are double-insulated with no protective earth at all (Appendix B). Counting X alone biases the estimate very slightly low.

Commercial equipment carries larger input filters: a variable-speed drive holds tens of VAr and upward, energised wherever the installation is left connected. The regulatory structure makes the accumulation one-way: one instrument drives the capacitance into practically every product—the filter is the universal compliance solution, not a named requirement—while, as Section I-A noted, no instrument bounds its fundamental-frequency injection—and a larger X-capacitor is generally the cheaper route to compliance. The filter's own earth-side element shows what recognition of an aggregating current looks like: leakage sums across everything sharing a protective conductor, and the regime bounds it at both scales—per device, through the touch-current limits that hold Y-capacitance to nanofarads, and per installation, where wiring rules hold a protected circuit's accumulated standing leakage to a fraction of its residual-current device's rating [32]. The X-capacitance's fundamental-frequency current aggregates just as surely—tens of devices behind a connection, whole fleets behind a grid exit point—but each device is certified alone, against a standardised artificial mains network, and the sum is, as far as we are aware, bounded at no scale by any instrument (Appendix B).

New Zealand's compliance instrument even encodes the two populations: since at least 2004 the EMC notice has assigned products incorporating switched-mode power supplies to a conformity level requiring a test report, while leaving wire-wound mains-frequency transformers at the lowest level [33]. Nor is the mandate the newcomer: the conducted-emission requirement has been the sole route to the European market since the start of 1996 [34] and a condition of sale in New Zealand since at least 2001, so the term's youth is the fleet's, not the rule's—what scaled through the 2000s and 2010s is the switched-mode population the rule reaches, while the wire-wound fleet those classes displaced carried no filter at all.

The hypothesis is disciplined by what it excludes: the large DC-link capacitor behind the rectifier makes no standing fundamental-frequency injection, being recharged through rectifier conduction pulses only while the device draws power; motor-run capacitors sit in series with the motor's auxiliary winding and are disconnected with it; and rooftop solar inverters contribute almost none overnight (the isolation relay strands the converter-side filter capacitors, leaving only a small grid-side element).

The last of those exclusions carries the most weight and is the one most open to challenge, since inverter topologies differ in where the anti-islanding relay sits relative to the mains filter and the photovoltaic fleet grew substantially inside the headline window. It is therefore bounded rather than asserted. Schedule 9e records distributed-generation connections made each year; summed over 2013–2025 the count is about 72,000, itself an over-count for photovoltaics because the series covers all distributed generation. At the top of the datasheet range for a mains filter (2.2 μF, 36.6 VAr) the whole fleet reaches 2.6 MVAr, or 0.7% of the 369 MVAr swing those grid exit points recorded. Granting the objection in full—the entire converter-side filter of a residential inverter, of order 10 μF, left energised on the grid side of the relay at every one of those connections—reaches 11.9 MVAr, about 3%. Night-time reactive modes at zero active power would sit on top of that, and are a real and growing mechanism (Section II-E flags exactly this at transmission scale), but they are dispatched rather than standing, and would not reproduce the connection-scaling signature of Section V-C on a fleet that reaches under a fifth of connections.

A bottom-up order-of-magnitude estimate—roughly two million households, each with 20–40 permanently connected filter-carrying devices at 2–4 VAr (the population above roughly 25 W: network, audio-visual, computing, and appliance electronics; published reference designs at or below 20 W carry no X-capacitor at all, and below about 25 W its presence is design-dependent rather than general (Appendix B); roughly 80–320 MVAr in aggregate), plus a commercial and industrial fleet of the same order—puts the national standing total at roughly 150–600 MVAr, or 100–200 VAr per household as the central band.

Sizing its most recognisable member bounds the composition: heat pumps were used in 66.8% of occupied private dwellings at the 2023 census, up from 47.3% in 2018—an adoption jump inside the study window, mostly at existing homes [35]—implying, at 1.2–1.6 units per equipped home, roughly 1.6–2.1 million residential units. Reference-design filter values for the outdoor units—the largest per-device contributors we found—are 1.4–2.0 μF each (23–33 VAr), putting the class at roughly 37–69 MVAr. Against the 80–320 MVAr residential envelope that is of order a quarter at central values: a material slice, but a minority, so the bulk of the standing term belongs to the far more numerous small supplies. Because the filter, unlike the heating duty, is energised year-round, the slice is also consistent with the drift's winter–summer invariance (Section III-B); a heating-season mechanism would not be.

The per-device values are physics and datasheet-grade figures, not New Zealand bench measurements—reference designs rather than teardowns of shipped New Zealand product—and the device counts are estimate arithmetic rather than a New Zealand census; we grade the attribution accordingly (component-level basis in Appendix B). The 20–40 band is anchored by the standby literature: 19 standby appliances per household across ten Californian homes in 2000 [36], and about 39 products per household in 2000 rising to 67 by 2005 in the Australian intrusive surveys [37]. The estimate's value is that it makes two testable predictions: the national scale of the drift, and—because the fleet lives behind consumer connections—that the drift should scale with the number of connections served, with nothing left at zero connections.

The first prediction is met at the order-of-magnitude grade the estimate carries. Summed across the same 114 grid exit points, the median overnight reactive power moved from $+188$ MVAr (net absorbing) in 2013 to -182 MVAr in 2025: a deepening of 369 MVAr (summarising each site by its 99th-percentile leading half-hour of the year, rather than its overnight median, gives 314 MVAr; the sites that deepened contribute 427 MVAr before the few that shallowed are netted off). Those exit points serve about 1.5 million connections, near 70% of the national total, so the rise normalises to about 210–280 VAr per connection on the footprint that produced it (209 and 285 on the two bracketing summaries above, 314 and 427 MVAr over 1.5 million connections, rounded inward)—above the estimate's 100–200 VAr per household centre rather than inside it. The gap is expected rather than anomalous, and Section V-C quantifies it: a connection is not a household, since the count includes commercial and industrial connections carrying larger filter fleets, and each connection also brings its share of medium-voltage cable. This is a bracket, not an allocation—the estimate bounds today's standing total, of which the twelve-year rise is the recently added part—and it is a bracket an order of magnitude wide by construction: what it can refute is a bottom-up estimate wrong by that much in either direction, and this one is not.

The dose arithmetic adds a third, cross-country prediction. If the filter is the mechanism, the per-connection drift should order across systems as ωV^2—Japan, then North America, then the 230-volt world—an ordering that cables, heat pumps, and correction plant have no reason to reproduce (Section VIII). The step from arithmetic to prediction carries one substantial qualification, and it is the reason this is offered as a test rather than a conclusion. The X-capacitor is not sized to a reactive-power target but to attenuate differential-mode conducted noise to a limit expressed in dBμV. For the same output power a 120-volt input draws twice the current and presents a lower source impedance, so the same limit demands more differential-mode attenuation, which a designer may buy with capacitance rather than inductance—North American designs can therefore need *more* X-capacitance, not the same, which offsets part of the V^2 dose. The offset is bounded by the same commercial logic that creates the fleet: a universal-input supply (90–264 V) is designed once and sold everywhere, and for that population the capacitance genuinely is chosen once and the mains sets the draw. The prediction is therefore strongest for globally traded universal-input product and weakest where a market gets its own design.

Every system in Section I-A runs 230-volt mains, and we are not aware of an equivalent North American measured report. We draw no inference from that: it is an absence of measurement, not evidence of absence, and North America differs from the systems in Section I-A in cable intensity, feeder topology, transmission voltage class and reporting practice as well as in mains voltage. The claim here is priority of measurement, not of exposure. The North American record the field does hold confirms the arithmetic rather than contradicting it: the documented North American case of overvoltage instability is Hydro-Québec's "highly capacitive" 735-kV network [12]—extra-high-voltage line charging behind 120-volt outlets, exposure in the network's voltage class rather than the mains-voltage dose. Of the two domestic predictions the second is the more discriminating; Section V-C tests it.

C. A connection-scaling test

Connection counts are public: the retail market-structure dataset on the same regulatory platform records the number of installation control points (ICPs—metered connections) behind each network supply point, monthly, from December 2003 [38]. We sum ICPs across retailers and embedded networks to each grid exit point, take calendar-year means for 2013 and 2025, and join them to the cohort under a documented correspondence audit, since the registry's root-NSP attribution and the metering's exit-point boundaries are not the same partition of the network: of the 114 sites, eight are direct-connect industrial points with no retail registry (a steel mill, a smelter, pulp and dairy plants), two lack a registry endpoint, one is unresolvable, and the remaining 103 all enter; sites whose registry codes demonstrably swap consumers with no matching movement of metered load (blocks of up to 27,000 move between neighbouring codes) are aggregated into station or sibling groups, giving $n = 96$ panel units. The test regresses each unit's 2013–2025 change in median overnight reactive power on the mean connection count it serves, against three criteria that follow from Section V-B's estimate and are recorded in the accompanying notebooks: the bootstrap 95% confidence interval on the slope excludes zero; the slope lies within 50–400 VAr per connection—the central 100–200 VAr per-household band widened downward because a meter records the net change rather than the gross filter capacitance added, and upward because commercial connections ride in the same count with more than a household's fleet; and the fit explains a nontrivial share (more than 15%) of the cross-site variance. A grid-exit-point-level metering artefact, with no mechanism to scale with the connections behind the meter, predicts the mean-only model instead (the same average change at every site).

The result is Fig. 5. The deepening scales linearly with connections served: the slope is -230 VAr per connection, the fit explains 80% of the cross-unit variance, and a through-origin fit agrees (-237). The panel's 96 units serve 1.52 million connections between them and sum to 376 MVAr of deepening, which the fitted line reproduces exactly: 348 MVAr from the slope plus 28 MVAr from the intercept. Section V-B's 369 MVAr is the lower figure because it nets off the sites that shallowed and spans all 114 exit points rather than the 103 that carry a retail registry. The coefficient belongs to this footprint and does not scale to the national connection count, whose connections sit partly behind excluded and contaminated exit points. Because sites under one company share an owner and are not independent, every interval here is reported under two resampling schemes, 4000 replicates each: resampling the 96 units independently gives a 95% interval of $[-272, -199]$, and resampling whole companies—the more demanding test—

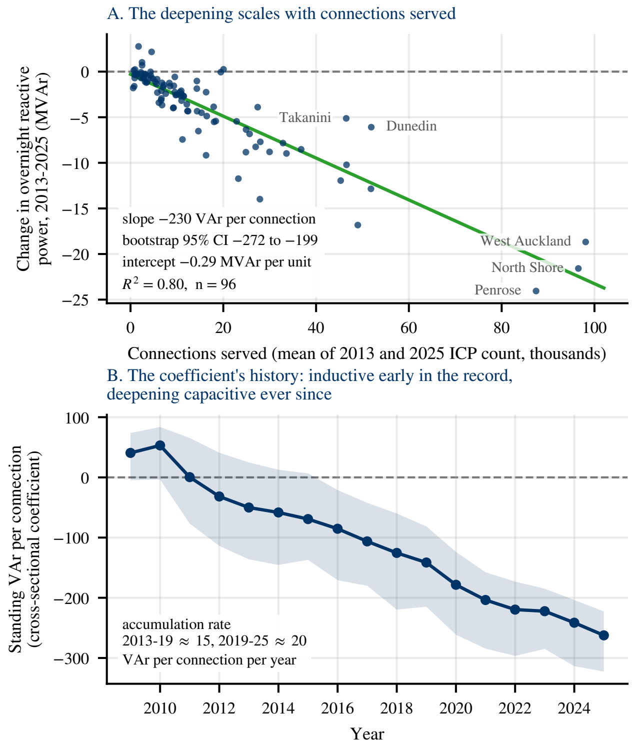

Fig. 5. The connection-scaling test. (A) Each screened panel unit's 2013–2025 change in median overnight reactive power against the mean number of connections (ICPs) it serves ($n = 96$): the change deepens at -230 VAr per connection (95% CI $[-272, -199]$ resampling units, $[-313, -209]$ resampling whole companies) with an intercept indistinguishable from zero (-0.29 MVAr per unit) and $R^2 = 0.80$ (80% of the cross-unit variance explained); deleting any single unit moves the slope only within $[-242, -220]$, and any single company only within $[-258, -224]$. Nothing about a grid-exit-point metering artefact predicts an effect proportional to the connections behind the meter. (B) The coefficient's history: the per-connection coefficient refitted across units each year on the 92 units present throughout 2009–2025 (shaded: bootstrap 95% CI). On the inductive side of zero early in the record, it crosses early in the 2010s—the intervals straddle zero either side of the crossing—and deepens every year thereafter at an accelerating rate. Sign convention: negative = added leading (capacitive) reactive power.

gives $[-313, -209]$, with a wild cluster bootstrap rejecting the no-scaling null at $p < 0.001$.

All three criteria are met, and the result is not fragile: a rank-based Theil–Sen slope agrees (-259), as does the unweighted mean of the units' own per-connection rates (-261); deleting any single unit moves the slope only within $[-242, -220]$ (removing the Penrose group—PEN0221 and PEN0331; PEN1101 is excluded by the Section II-E screen—whose position pulls hardest on the fitted line, moves it to -220, a 4% shift with the verdict unchanged), and deleting any single *company*, which removes several high-leverage units together, moves it within $[-258, -224]$. The high R^2 is not a size artefact: each unit's own VAr-per-connection shows no material dependence on its size ($R^2 = 0.001$). The mean-only artefact model loses by an Akaike information criterion (AIC) difference of about 155, a decisive margin on the standard model-selection score; that difference assumes independent units, and the wild cluster bootstrap is its clustered counterpart.

A mean-only null is, however, the weak null: nobody proposes that every site changed by the same absolute MVAr.

The null that matters is site *size*, because both axes scale with it, and the discriminating question is whether the change follows connections or follows load. We therefore run the two against each other in one specification, with each unit's overnight and evening-peak real power built on the same parquets, windows and aggregation rule as ΔQ (members summed per half-hour first, then the median, then the mean of the 2013 and 2025 values). Connections win on every reading. Alone, connections explain $R^2 = 0.80$ against 0.72 for overnight load and 0.76 for peak load, and beat both decisively on AIC (149.0 against 184.9 and 166.9). Added to connections, neither load term earns its parameter: R^2 moves 0.804 to 0.806 and AIC *worsens*. In the joint fit the connection term holds a bootstrap interval clear of zero (-200 VAr per connection, $[-127, -297]$) while the overnight-load term's spans it ($[-0.1, +0.1]$ MVAr/MW). The collinearity is real but not disabling: $r = 0.92$ between connections and overnight load, a variance inflation factor of 6.7 on each, below the conventional threshold at which a joint fit stops being readable.

The fit is also visibly anchored by four or five high-leverage units at the right-hand end, so we report the leave-the-top-five-out coefficient explicitly. Dropping West Auckland, North Shore, Penrose, Dunedin and Wellington—the five largest by connections served—*raises* the slope from -230 to -261 ($[-207, -316]$, R^2 falling to 0.69 as the range is removed); dropping the top ten gives -291 and the top twenty -279. The high-leverage points hold the coefficient *down*, not up, so the result is not manufactured at that end.

The intercept—what is left at zero connections—is -0.29 MVAr per unit and indistinguishable from zero under every inference scheme: resampling units gives $[-0.74, +0.21]$, resampling whole companies gives $[-0.65, +0.52]$, and the wild cluster bootstrap retains the no-intercept null at $p = 0.29$. Aggregated across the 96 units the point estimate is -28 MVAr, under a tenth of the cohort's 369 MVAr deepening. The bottom-up estimate predicted nothing at zero connections; the measurement meets that prediction on both limbs. The first run under the same criteria, on the narrower 83-site screen panel that predates the correspondence audit, reads -253 (CI $[-291, -192]$, $R^2 = 0.77$): the same verdict, agreeing with the audited panel to within about 10%; we report both, never blended. A two-term variant separating existing connections from connections added over the window cannot split them on this panel: the two counts are strongly correlated across units and the added-connection term's interval spans zero, so the accumulation-versus-growth question falls to the coefficient's history below.

The coefficient also has a history (Fig. 5B). Refitting the across-units regression year by year on the 92 panel units present throughout 2009–2025—each year on the standing level rather than the 2013–2025 change, so the coefficient carries the whole connection-scaling class—the per-connection term starts on the *inductive* side of the axis (+41 VAr per connection in 2009, the motor-era fleet's residual signature), crosses zero in 2012, deepens every year thereafter, and reaches -262 VAr per connection by 2025. The crossing year is a point estimate: the yearly intervals straddle zero on both sides of it, and the interval is clear of zero on the capacitive side only from 2016, so the ramp and the post-2016 deepening are what the data establish, not the date. The 2013–2025 movement, -212 VAr per connection, reproduces the two-endpoint slope within 10%. That is a consistency check across two parameterisations of the same metered panel, not corroboration by an independent route: it establishes that the result does not depend on whether the coefficient is fitted to the endpoint change or read off the level history.

The in-window accumulation rate rises across the window (about 15 and 20 VAr per connection per year over 2013–2019 and 2019–2025, the 2009–2013 span being the crossing itself)—a comparison of two window means on serially overlapping data, reported without a test on the difference; and the series is smooth, where a staggered metering-replacement artefact would enter as steps (the largest single-year movements, over 2019–2021, coincide with the pandemic years). The emergence also overlaps the 2010–2013 meter-fleet replacement (Section II-C), and the coincidence is worth naming: an instrumentation change would enter as a step to a new level, not as a ramp that crosses zero mid-record and is still deepening a decade after the rollout ended, equally in both diurnal windows, and concentrated in the term that scales with connections. The connection-scaling structure, in short, is not a fixture of the network: the fleet's per-connection signature swept from inductive through zero early in the 2010s and is still steepening on the capacitive side. We do not attribute the crossing date to any single device class.

The inductive starting point has a domestic witness: the national household end-use project metered real and reactive power in nine houses over 2002–2004 and found the always-on standing load at a power factor of 0.5–0.7 inductive, attributed to motors and "transformer inductive loads" [39]—the iron fleet this record watches leave—while dismissing the era's small chargers on a watts-only basis ("less than 0.5 W"). Two caveats travel with it: nine non-randomly selected houses, on the project's own caveat; and its power factor is a total rather than a displacement quantity, so at the harmonic-rich currents of early switch-mode standby a low value need not indicate inductive displacement, and the inductive reading rests on the load classes the project identified rather than on a sign measurement at the fundamental. It corroborates the starting point; it does not measure it.

Read honestly, the slope is the whole connection-scaling shunt class, not the device fleet alone. Each connection also brings its share of medium-voltage cable (low-voltage cable is negligible, since charging scales with V^2), and commercial and industrial premises hold the one rival source of standing capacitance at scale: power-factor-correction banks, installed against peak lagging demand and—because correction is fitted for the lagging problem, never its mirror—left in service overnight wherever the control is fixed or coarsely stepped. The scale gap is the threat: a single commercial building's stranded bank (tens of kVAr) outweighs its own device fleet twenty-fold or more, so a slope carried by commercial connections would break the device attribution even with the scaling law intact.

The registry separates the populations. Every connection carries an industry classification (residential connections carry none, ANZSIC divisions A–E are industrial, F–Z commercial), published per root NSP—the same key the panel's counts already join on. The registry file is published as a rolling snapshot, so its history was recovered from the Internet Archive's Wayback Machine: twenty-five date-stamped vintages, December 2018 to October 2025, plus the live July 2026 file; a logged search found no earlier vintage anywhere, so class-resolved history begins December 2018 (and no 2021 vintage exists). Splitting each unit's count into its residential and commercial-industrial parts—class counts averaged over the eight registry year-marks—and fitting one coefficient to each puts the residential coefficient at -147 VAr per connection (95% CI $[-240, -81]$ resampling units, $[-329, -86]$ resampling whole companies)—on the 86% of connections that hold no correction plant at all—and the commercial-industrial coefficient at -915 ($[-1392, -299]$ units, $[-1288, -98]$ companies): larger per connection, as commercial device fleets and shared cable predict. On these point estimates the two classes carry about half the panel's 376 MVAr of deepening each—192 and 195 MVAr, a pair that sums a little above the panel total because the two-class fit carries its own intercept—despite the six-to-one difference in their numbers, the commercial-industrial share running from 17 to 79% across its own interval. That term is not decomposed here: commercial device fleets, any stranded correction, and shared medium-voltage cable all sit inside it, and its magnitude alone does not separate them. The two counts are collinear across units ($r = 0.94$), so the split is read as bounds rather than a sharp allocation; single-vintage fits (December 2018: -135/-1011; July 2026: -158/-853) and deleting the largest units move the coefficients without changing any verdict. And because the residential class is defined by the absence of an industry code, any miscoded commercial connections sit inside it and deepen its coefficient, so the true household figure is if anything lower.

The units that sit off the fitted line do so in a sensible pattern: grid exit points serving industrial-weighted load (Takanini and Wiri, in south Auckland) deepen less than their connection counts predict, while the Penrose group, serving Auckland's cable-dense inner isthmus, deepens more.

Two marks bear on the correction reading, and a third that might have been expected to does not. First, correction plant loads the level, not the drift: as with the distribution capacitor fleet of Section VI-B, a static stranded stock cannot produce a deepening trend, and the population able to hold a bank—current-transformer-metered connections—grew by about 3,100 sites between December 2018 and July 2026, 1.7% of this footprint's connection growth over the same span (registry class snapshots begin December 2018, so this leg covers the record's back half rather than the full window). For stranded correction at new sites alone to carry the commercial-industrial term, each of those sites would have to hold some 60 kVAr of permanently connected, never-switched compensation. Second, the class's own standing level is still net lagging in every matched year (Fig. 6): a population dominated by capacitors left in service would read leading, not absorbing. Third, and reported because it is the test that looks decisive and is not: the per-connection deepening is statistically flat across units ranked by commercial-industrial share (pooled rates by tercile 233, 280 and 228 VAr per connection), but the share coefficient's interval is wide enough to contain the concentration the split itself implies, so the flat reading is consistent with the split rather than evidence against it. The unmasking channel—static banks exposed by falling overnight commercial load—does run against the measured record, since overnight demand at these boundaries rose over the window (Section IV-C). What the split leaves unresolved it bounds: within the commercial-industrial coefficient, commercial device fleets, any stranded correction, and shared cable remain unseparated; within the residential coefficient, the split of -147 VAr between device filters and per-connection cable remains hypothesis-grade. Whichever way those compositions fall, the term stays demand-side and connection-scaling: correction plant behind a connection is not network cable, so its presence would qualify this section's device-layer attribution rather than the decomposition of Section IV.

The standing level completes the picture (Fig. 6). Refitted each year on matched vintages, the residential level runs from -247 VAr per connection in 2018 to -310 in 2025, leading in every year with the interval clear of zero. That level, and not the twelve-year change, is the quantity the bottom-up estimate of Section V-B predicts, and it lands *above* the 100–200 VAr per-household band rather than inside it. It should: the level carries each connection's share of medium-voltage cable as well as its devices, and Section IV-C's charging physics puts that share at roughly 190 VAr per connection nationally (454 MVAr computed for 2025 over 2.34 million connections), which is the order of the gap. The arithmetic is a consistency check between two independent computations in this paper, not a decomposition: it allocates nothing, and the residual inductive limb of Section V-A sits inside it. Meanwhile the commercial-industrial level runs from about $+858$ VAr per connection—net *lagging*—down to $+111$ by 2025, its interval spanning zero throughout. As a class, commercial and industrial connections still absorb more overnight than they inject; the margin has fallen by roughly three quarters since 2018, but the crossing the residential class made years ago has not yet happened there. That standing position is itself evidence against the stranded-correction reading of the class's fast per-connection change: a population whose overnight signature is still net lagging is not one dominated by capacitors left in service, and part of its change is the overnight motor and process load leaving—the same departure of the inductive fleet the record shows economy-wide, one class up. One registry artefact travels with the series: a reclassification batch of roughly fifteen thousand connections moved into the commercial-industrial class between the February and March 2020 vintages, visible in Fig. 6(B); it sits inside the class series without changing the direction of either.

The scaling is also not site size in disguise. Load and connections rise together across sites, so a load-proportional metering error—the $P \sin\beta$ class of Appendix A—would mimic connection scaling; but that class is bounded far below the measured deepening, would concentrate the deepening in the loaded window rather than equally in both (Section V-A), and would over-predict precisely the industrial-weighted sites that in fact fall short of the fitted deepening.

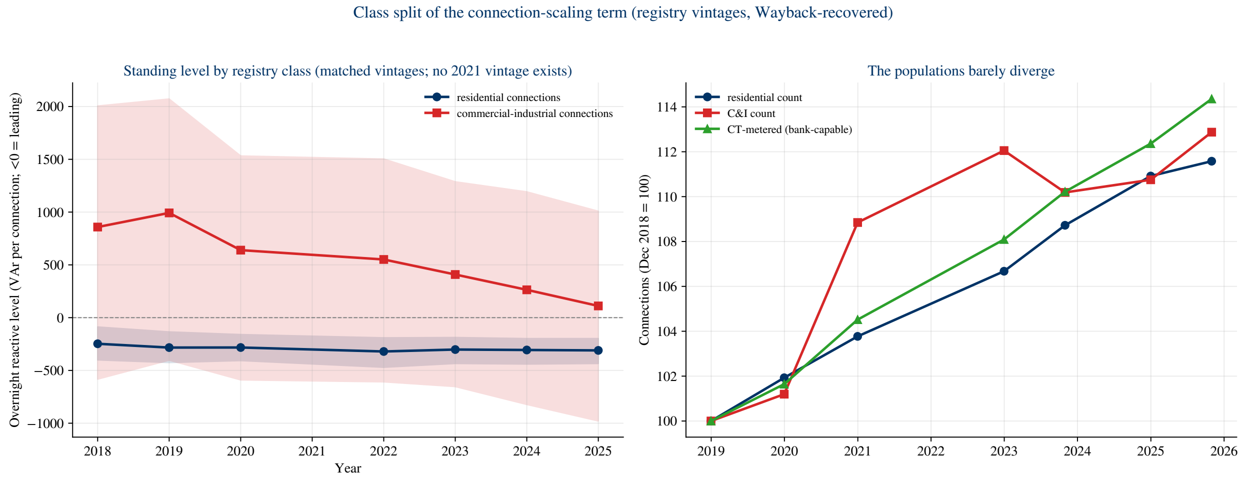

Fig. 6. The connection-scaling term split by registry consumer class. (A) The standing overnight reactive level per connection, refitted each year on that year's own registry vintage: the residential coefficient is leading and deepening in every year, its interval clear of zero; the commercial-industrial coefficient descends from net lagging toward zero and has not crossed it, its interval spanning zero throughout. No 2021 vintage exists; bands are bootstrap 95% intervals resampling units. (B) The class populations, indexed to December 2018, with the current-transformer-metered (bank-capable) population: near-parallel growth, no commercial tilt in the mix. Registry vintages December 2018–July 2026; superseded vintages recovered from the Internet Archive.

One rival survives in principle: a load-independent metering-registration drift phased in with meter replacement. It has no mechanism to produce the connection-scaling term that carries the deepening, and the connection-independent residual it could sit in is indistinguishable from zero under every inference scheme, so it is heavily disfavoured as an account of the trend while remaining formally excludable only by a measurement that bypasses the grid-exit metering chain. That measurement is identified and simple—night-time reactive flow at a residential distribution transformer with a known house count, where metering on the low-voltage side sees no transformer magnetising and no material cable charging, isolating the device fleet and splitting the coefficient—and is the stated next step.

VI. From Leading Reactive Power to Overvoltage

A. Why leading reactive power raises voltage

The relationship to hold in view is that the voltage change along a line depends mostly on the reactive power and the reactance, $\Delta V \approx (RP+XQ)/V$, with the XQ term dominant on the grid. When reactive power is lagging ($Q > 0$, the historical norm) voltage drops toward the load, and networks were designed around this with tap-changers and capacitors to prop voltage up. When reactive power is leading ($Q < 0$, the new overnight reality) the sign flips and voltage is pushed up. Light load is the dangerous condition because demand is lowest—so little load absorbs the reactive power or pulls voltage back—while the cable charging is always on. The mechanism can run away: charging rises with the square of voltage, so a higher voltage injects more leading reactive power and raises voltage further, and a protection trip that disconnects a transformer or load leaves the remaining network carrying more charging per unit of load, stressing the next element in turn. Two distinct feedback loops run through that description, usually described as one (Fig. 7). In the first, the *demand-side* loop, disconnected load takes with it whatever reactive absorption it was providing, and voltage rises; whether shedding load raises voltage or lowers it therefore turns on the power factor of what comes off, since lagging load removes absorption while sufficiently leading load removes a reactive source instead. In the second, the *plant-side* loop, rising voltage disconnects plant and generation that were absorbing, and voltage rises further; that loop runs on the response of protection to voltage and would run the same way behind a demand of any power factor. In isolated and autonomous systems the feedback is well documented [40], [41]; in neither 2025 blackout did the lost absorption leave with the demand (Section VI-C).

B. The system is already responding

The New Zealand system is visibly responding to overvoltage pressure from both ends.

Distribution capacitors are coming out. If networks were suffering low voltage they would be adding capacitors, which raise voltage; instead they are removing them. From the Commerce Commission disclosures, the national capacitor-bank count fell from 298 in 2015 to 254 in 2025, and the largest network removed 47 of 104 banks over the same period. The series is counts only and shows direction, not MVAr, but the direction is the point: a static-to-shrinking capacitor fleet cannot be causing a rising leading trend, and the removals are the signature of the opposite, high-voltage problem. One confound the count cannot see should be named: the quantity that would matter is not the stock but the operating practice—banks once switched out overnight and now left in, or the reverse—and a switching schedule maps one-for-one onto the residual while leaving the count untouched. No public series records it. The constraint on it is the connection-side evidence of Section V-C rather than this count: the population able to hold a bank accounts for 1.7% of recent connection growth, the

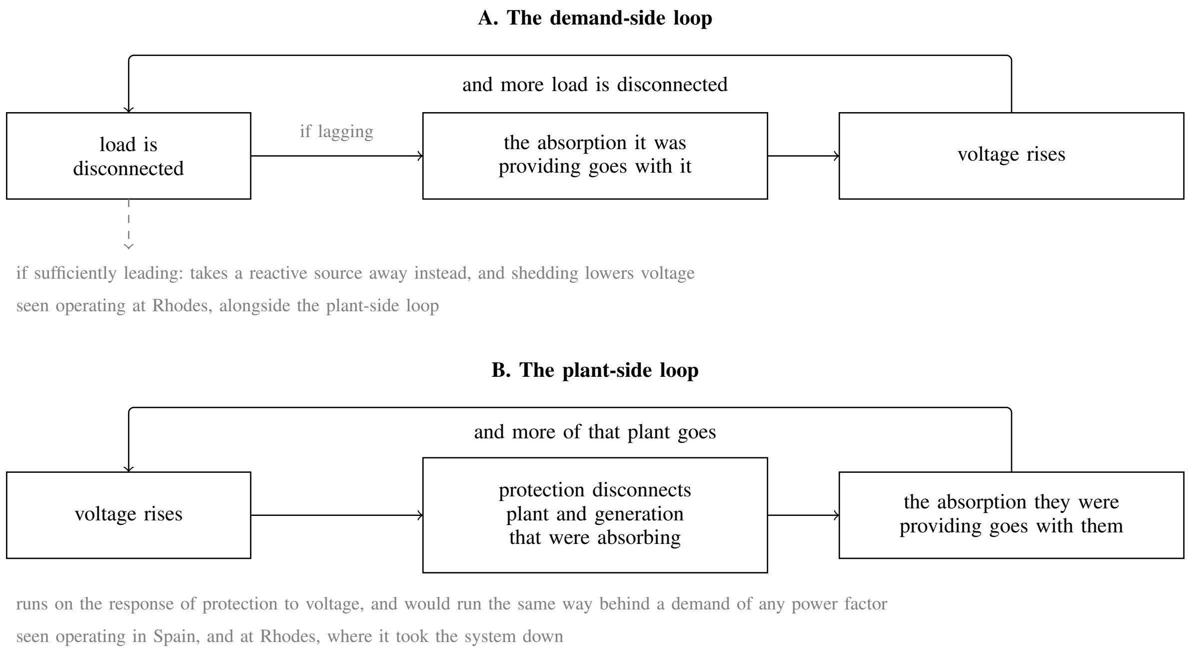

Fig. 7. The two feedback loops. In the demand-side loop, disconnected load takes the absorption it was providing with it and voltage rises; whether shedding load raises voltage or lowers it turns on the power factor of what comes off, which is the quantity Section III measures moving. In the plant-side loop, rising voltage disconnects plant and generation that were absorbing, and voltage rises further; that loop runs on the response of protection to voltage and would run the same way behind a demand of any power factor. Spain ran on the plant-side loop. Rhodes ran on both, the plant-side loop taking the system down and the demand-side loop making the voltage worse on the way. In North Macedonia there was no compensation plant to lose and no load was shed at all—the demand-side loop never operated (Section VI-C).

residential class that holds none carries its own coefficient, and the commercial-industrial class remains net lagging overnight in every registry vintage.

Transmission reactors are going in. Shunt reactors absorb leading reactive power, and the grid operator has been installing them in the Upper North Island (Table IV). Its System Security Forecast records both the practice and the remedy: "[o]vernight high voltages are currently managed by removing selected transmission circuits from service," and the two 100 Mvar Pakuranga reactors "will dramatically reduce the number of circuit switching operations required to manage high voltages under N-1 conditions" [42]. The operator's follow-up study confirms the outcome: with the Pakuranga reactors and the Hamilton STATCOM in service, "significant over-voltage issues have not been observed for current and future light load conditions" [43]. The investments, and the operator's own description of them, are consistent with managing an overnight overvoltage condition. (A further dynamic device, a Henderson STATCOM, is proposed under the WUNI Stage 2 major capex proposal but not yet approved.)

And the operator has named the demand-side term. Transpower's 2023 transmission planning report records that keeping lower North Island voltages within limits at light load "requires high levels of reactive power absorption from the Haywards synchronous condensers," and that "HVDC transfer may also be limited for harmonic performance if the number of filters must be reduced to prevent high voltages"; it expects the high-voltage issue to worsen, and lists "load characteristics becoming generally more capacitive" among the factors [44]. That is the asset owner, in a planning document, attributing part of the standing pressure to the electrical character of the load—the quantity this paper measures.

TABLE IV
UPPER NORTH ISLAND SHUNT REACTIVE COMPENSATION, IN SERVICE (RATINGS FROM TRANSPOWER'S INTERCONNECTION ASSET CAPACITY DISCLOSURES AND PROJECT RECORDS)

Asset	Rating	Status
Otahuhu reactor R472	50 MVAr	2022
Pakuranga reactors R562, R582	100 MVAr each	2023
Wairau Road reactor R182	63.7 MVAr	in service
Hamilton, Otahuhu STATCOMs	dynamic	2023–2025

C. The realised risk, abroad

The regime is not hypothetical. The Iberian event of 28 April 2025 was found to be a voltage and reactive collapse: the Final Report identifies "non-effectiveness of voltage control" as a root cause; we read it as placing the system's inability to manage a capacitive excess at the centre of the failure, and it does not attribute the event to insufficient inertia [16]. The absorption the cascade removed left with the generation: generators tripped on overvoltage protection, each disconnection taking its reactive absorption with it, and the under-frequency load shedding acted only after the generation trips had run their course—the Final Report finds the scheme delayed the collapse rather than hastening it, while noting it was not designed for a system in widespread overvoltage [16].

The North Macedonia event of 18 May 2025 was a cascade of transformer trips from sustained overnight overvoltage, driven by the high capacitive reactive power of light-load transmission and distribution networks, with the running wind plant injecting rather than absorbing and no compensation plant on the system at all—so the cascade needs neither solar nor distributed generation—and with no load shed: the demand went only at the end, when the last 400/110 kV transformer tripped, so the cascade ran with the demand-side loop never operating [17]. Each event had local specifics; we read them as corroboration that the leading-reactive regime is a realised blackout mechanism, with New Zealand's distinctive contribution the 29-year measurement and decomposition of how a system drifts into that regime in the first place.

D. Coverage of existing reactive-power provisions

New Zealand's reactive-power rules were written for the old problem of lagging load pulling voltage down at the daytime peak. The connection minimum power factor is a term of the default transmission agreement that binds the distributor for the aggregate power factor at the connection point—the right party, at the boundary where Section III takes its readings—but it applies during regional peak demand periods and at no other time, the periods themselves fixed by reference to a transmission pricing methodology replaced in 2023 [45], so the one window where overvoltage now lives is the window the rule does not cover; the reactive-demand measurement provision operates only on weekday hours, 07:00–21:00 [46]; and where lines companies charge for power factor, the published schedules charge on a lagging basis (e.g., [47]). We are careful about what this does and does not mean. The rules did not *cause* the leading surplus: Sections IV and V show the driver is the product-standard demand fleet, outside the rules' reach, and Section VI-B shows the capacitor fleet is shrinking, not the legacy of an over-correcting rule. What the existing provisions do is not cover, price, or limit the leading reactive power now accumulating overnight. Whether that coverage should change is a policy question outside this paper's descriptive scope; the descriptive finding is the measurement, and we note the policy question without arguing it.

One rule moved as the record closed: on 13 November 2025 the statutory low-voltage supply band was widened from 230 V $\pm 6\%$ to $\pm 10\%$ [48]. Because each data year here is a whole calendar year, about seven weeks of the 2025 endpoint sit after commencement rather than before it. The exposure is small, confined to the last weeks of a twenty-nine year record, and runs with the reported drift rather than against it; but the measurement is not strictly pre-commencement and we do not claim it as such. The widening bears mechanically on what follows. Standing capacitance draws $Q = \omega C V^2$, so the same fleet delivers about 2% more reactive power for each 1% of sustained voltage elevation the wider band accommodates: some 8% more at the new ceiling than was possible at the old one, and about a fifth more than at nominal voltage. A band that previously forced intervention as light-load voltages rose no longer does. Post-2025 updates of the per-connection coefficient should therefore either control for measured voltage or name the confound: to the extent that light-load voltages rise into the new headroom, part of any further deepening is voltage-induced rather than fleet growth.

VII. Implications for Power-System Analysis

The measured reversal relocates the binding voltage-security question. For the lagging era's failure mode—voltage collapse under heavy load—power-system practice holds a mature, layered stack: automatic under-voltage load shedding as a last resort, tap-changer blocking, PV- and QV-margin analysis, and decades of operational tooling, all built on load models of an inductive fleet. In the light-load regime—overnight here and in North Macedonia, and the middle of the day on systems where distributed photovoltaics hollow out net transmission demand—the equivalent layers are thinner in three places: the compensation provision was sized by voltage level for the old direction, the *automatic* last-resort layer acts on voltage falling, not rising, and the margin tooling reports distance to collapse, not to the upper limit. We take those three in turn, add the load-model correction the measurement makes concrete, and close with its honest boundary.

The first is a question of what was installed, not of what drives the surplus. The surplus is made at the mains and appears at every level above it, but what stands against it was installed for the old direction. The extra-high-voltage network already carries the switchable reactor fleet its own line charging obliges, and that plant absorbs a demand-side surplus arriving from below as readily as it absorbs its own. The levels between were built for the opposite problem—lagging load pulling voltage down at the daytime peak—and what stands there is capacitor banks. The exposure is thinnest there, and that is where a search should start. It is not a claim that the extra-high-voltage network is covered: both 2025 events occurred there, driven by the network term that dominates at that voltage.

The second is the standard emergency lever, built for the falling direction; in this regime its effect on voltage is no longer of one sign. In a collapse, shedding load is corrective: every megawatt shed relieves the stress that is depressing voltage. In the light-load capacitive regime the two loops of Section VI-A separate. What shedding does to voltage in the demand-side loop turns on the power factor of what comes off—lagging load takes absorption away with it; sufficiently leading load takes a reactive source away instead—and that power factor is the quantity Section III measures moving through zero, so a scheme designed on the lagging assumption can no longer assume it. The plant-side loop is indifferent to what the demand draws—protection that removes absorbing plant raises voltage behind a demand of any power factor—and it is the loop the Iberian cascade ran on; in North Macedonia the demand-side loop never operated at all (Section VI-C).

In the Iberian event the voltage kept rising as the under-frequency stages acted, for reasons the Final Report locates in the network and the generation rather than in the shed demand: the shedding reduced line currents, leaving higher residual voltage and more line charging, while the simultaneous disconnection of generators reduced voltage control and absorption [16]. The Rhodes cascade of 2016 is the one investigated event in which the demand-side loop can be seen operating: under-frequency shedding raised voltage and deepened generator reactive absorption—an aggravator in a collapse ultimately triggered on loss-of-field, and one a small shunt reactor would have prevented [40]—and rerunning the disturbance with fewer shedding stages avoids the overvoltage while holding the same frequency nadir. No investigated event attributes a blackout to the demand-side loop. And on the demand character measured here the implication runs further: net-leading demand takes a reactive source with it when it trips, so the classic load-rejection voltage rise weakens and can reverse in sign, and the overvoltage exposure in an event concentrates on the plant side—the absorbing plant and generation that protection removes, and the under-excited operating points where the autonomous-system record already places the failure path and its countermeasures (under-excitation limiters blocked for isolated generators feeding capacitive networks; any voltage-setpoint change made in the absorbing direction) [40]. The last-resort schemes discussed here were all designed for the other direction: none connects load or absorption when voltage runs away, and none reads the power factor of what it sheds.

Two things about the surplus bear on that second leg. The distinction between the drift and the level matters here (Section IV): the *drift* into the regime is dominantly the demand fleet, but the standing light-load surplus the mechanism feeds on is substantially long-standing distribution network charging that the fleet's shift has uncovered—distributed, always energised, scaling with the square of voltage (Section VI-A), and not itself dispatchable, since its removal means switching circuits out of service, spending N-1 security to buy voltage margin (Section VI-B). The cascade arithmetic is then inverted relative to collapse: each element lost in a voltage collapse—a stalled motor tripping, load disconnecting—reduces the demand that is depressing voltage, so the disturbance partly self-relieves, whereas in the plant-side loop each definite-time protection operation removes absorption and strengthens the driver, so the disturbance self-reinforces in quantised, irreversible steps—the arithmetic of both 2025 events (Section VI-C). The Iberian sequence ran from first protection operation to blackout in well under a minute [16]; the North Macedonian event shows the same physics grinding through a lightly compensated system over hours [17]; the autonomous-system literature finds the positive feedback sharpest in small and weakly interconnected systems [40], [41].

The third is the margin tooling. Overvoltage protection and locally automatic shunt switching exist as device-level controls, and the QV curve's upper limb, temporary-overvoltage studies and self-excitation screening each address part of the question; but none is reported as a routine margin quantity the way PV and QV margins report distance to collapse, and the field's 2026 mechanisms review likewise proposes containment countermeasures for the upper band without proposing a margin quantity for it [12].

The analysis stack under-represents the regime it is entering. Planning and protection studies still commonly represent demand with constant, lagging power-factor archetypes calibrated to the motor-dominated fleet, and expert reviews have already documented the error constant-power-factor load modelling introduces [7], [8]; the measured net overnight flow now carries the opposite sign, so the studies most responsible for revealing the risk are calibrated to a fleet that no longer describes the night. That reaches past the archetype: by the sign argument above (Section VI-A), a shedding or load-rejection study calibrated on lagging demand carries an unexamined sign at light load. The gap is calibration rather than structure. The standard composite load model does carry a distribution-side shunt term—but not as an inventory of plant: its value is computed at initialisation "to balance the reactive consumption of the load devices and of the transformer and feeder with the load Q value specified in the power flow data", and it is then allocated across the load components in proportion to each one's share of megawatts [49]. The model therefore inherits whatever reactive character the power-flow case carries, and at light load—the condition such cases have least often been built against a measured demand character—it reproduces a lagging archetype as though it were measured plant. Where demand is then lost by tripping whole feeders—under-frequency or interruptible-load schemes—the capacitance behind them is genuinely de-energised with them, so removing it is correct in direction, and the megawatt weighting is second-order: a large representative block sheds connections and megawatts in similar proportion. Only where a device stops drawing while its supply stays live—the specification's end-use protection case, in which the allocated capacitance is "tripped in proportion to the MW of each component tripped"—does the removal run against the physics. The sequence matters as much as the mechanism. Under-frequency and interruptible-load schemes act on frequency, so in a voltage-led disturbance they operate only once enough plant has been lost to move it: of the three investigated events, one shed no load at all and in another the absorption left with the generation (Section VI-C), while in the third shedding aggravated a collapse already running on loss of field (Rhodes, above). What the demand contributes at initiation is therefore a standing level rather than a trip—and the standing level is the part the initialisation inherits rather than measures.

The measurement gives the load-model correction a concrete, portable form. The light-load fleet needs a net standing shunt term that scales with connections served—on the New Zealand panel, about 230 VAr per connection accumulated over 2013–2025 (Section V-C; a boundary-level figure that carries each connection's share of network cable with it)—alongside whatever power-factor archetype represents the operating draw. A constant-power-factor archetype cannot represent this term even qualitatively: it is present when the load is not drawing; it accumulates behind existing connections rather than arriving with demand growth—the coefficient of Section V-C is fitted per connection and refitted each year, so a fleet growing only in step with new connections would leave it flat, whereas it swept some 300 VAr per connection across the record—so it will not surface in load forecasts either; and it is young and moving—on the inductive side of zero early in the 2010s, accumulating faster over the second half of the window than the first (Section V-C)—so archetypes calibrated even a decade ago predate the term entirely.

None of this makes the regime unmanageable. With fast absorption installed, New Zealand's operator reports no significant overvoltage issues under current and future light-load conditions (Section VI-B): what is missing is not feasibility but architecture—the compensation provision, the automatic defences, the security-margin tooling and the load models were all built for the direction the system has left. Their redesign is development work beyond this paper's descriptive scope. What the measurement supplies is the direction and the rate: a national boundary flow that has crossed to the capacitive side of the axis around which those tools were built, driven dominantly by the load fleet, at about -0.018 MVAr per MW of overnight load per year, with the crossing already behind it.

VIII. Future Work

The measurement opens more questions than it settles. We collect here the ones it makes tractable, several of which consolidate pointers made throughout.

The attribution measurement. The first priority is the decisive test named in Section V-C: night-time reactive flow at a residential distribution transformer with a known house count, which isolates the device fleet from the per-connection cable share, complemented by bench measurement of the standing injection of common device classes in standby. One instrumented night and one instrumented bench would move the central hypothesis of Section V-B from labelled to tested.

How long can it run? The coefficient's history (Fig. 5B) shows acceleration, not saturation. A single adoption curve must eventually saturate, but the fleet is a *succession* of curves—lighting, broadband equipment, heat pumps, and next an electric-vehicle charging and home-battery fleet expected to carry the largest input filters yet—so extrapolation calls for a renewal model of device generations—each wave layered on and later replaced—rather than a logistic (single saturating S-curve) fit to the total. Bounding scenarios (the present $\sim$20 VAr per connection per year held constant; saturation at the current device census; the vehicle wave layered on top) built from appliance-stock and sales data would bracket the 2030s trajectory. Nothing in the record yet marks the turn.

Whether any instrument should see it. The standing term currently falls outside every instrument that could notice it: asset registers, load models, demand forecasts, product standards (Section I-A), and reactive-power provisions written for lagging daytime load (Section VI-D). Whether any of them should see it—and at which level: product standard, connection requirement, or network tariff—is a question of standards development and regulatory economics beyond this paper's descriptive scope. We note only that the relative economics of absorbing the surplus at the grid level against not creating it at the product level appear to be unquantified in the open literature, and that the quantity now accumulates at a measured, forecastable per-connection rate.

Power-system analysis. Four concrete developments follow from Sections V and VII: a connection-indexed net standing shunt term and its placement within composite load-model structures; a routine margin quantity for the upper voltage band—distance to capacitive runaway—analogous to the PV and QV margins of the collapse toolkit; the frequency-domain counterpart, since distributed shunt capacitance reshapes the network's harmonic impedance as well as its fundamental-frequency balance—if the term accumulates behind every connection, the parallel resonance a network presents to the transmission system falls year on year toward the low-order harmonics, which is a screening quantity the same measurement supplies and no part of this paper's fundamental frequency analysis addresses; and the automatic last-resort defence architecture for the overvoltage direction, whose absence Section VII records (the 2026 review proposes transmission-level elements of one—tap-changer blocking on instability detection and emergency converter reactive absorption above 1.08–1.10 pu [12], [50]—leaving the demand-side term itself unaddressed).

Replication and the meter fleet as instrument. The test needs only settlement metering and connection counts, so any operator can reproduce it; comparative axes of interest include heating-electrified against gas-heated building stocks; systems whose device adoption leads New Zealand's, such as Norway's vehicle fleet; and the mains-voltage axis itself, since if the filter is the mechanism the per-connection drift should order as ωV^2 from Japan through North America to the 230-volt world (Section V-B). And where advanced meters record reactive energy at the connection itself, the per-connection term could in principle be read directly and continuously from the metering fleet, closing the chain from device to grid without new instrumentation.

Separating the two limbs. Section V-A establishes that the measurement returns $Q_L - Q_C$ and never either limb. Two routes could split it, and neither needs new field instrumentation. The first anchors the inductive limb at the start of the record: the national household end-use project metered real and reactive power in nine houses over 2002–2004 and found the always-on standing load at 0.5–0.7 power factor inductive [39]; if its standing real power per house is recoverable, $Q_L = P \tan\phi$ converts that directly into a starting level in VAr per household, against which the level history of Fig. 5B could be read as a retreat. Its caveats (Section V-C) apply: nine non-randomly selected houses, and a total rather than a displacement power factor. The second is frequency sensitivity, which returns the *sum* where the level returns the difference: $Q_C = \omega C V^2$ rises with frequency while $Q_L = V^2/\omega L$ falls, so at fixed P, $\mathrm{d}Q/\mathrm{d}f = -(Q_L + Q_C)/f$, and two equations resolve two unknowns. Feasibility is the open question and should be scoped before the method is relied on: half-hourly averaging smears frequency excursions to perhaps ± 0.05 Hz of usable variation, the load's own frequency response in P and Q confounds it, and what it returns is the total system L and C including cable charging and transformer magnetising, from which Section IV-C's computed cable term would have to be subtracted.

A fitted circuit model. A companion study, in preparation, fits the circuit form directly: a standing term with drift and dated operational steps, load-composition and series terms, and embedded-plant signatures, fitted at every grid exit point and validated element by element against dated network events, connection counts, and metered embedded generation.

IX. Conclusion

Using 29 years of regulatory half-hourly metering, we measured a national power system's reactive character shifting from lagging to leading at supply-point resolution: on the balanced demand panel (the same 123 grid exit points throughout), mean overnight reactive power fell from about $+466$ MVAr to about -451 MVAr (about -31 MVAr/yr), crossing net-leading overnight in 2016 and at the evening peak only later—a measured phenomenon, not a metering artefact, holding in winter and summer alike, within the modern metering-fleet era alone, and with every contaminated grid exit point removed. The drift is dominantly the demand side: a first-principles charging calculation that fits no cable coefficient puts the organic share at about 80% (physical band 75–88%) over the 2013–2025 asset-disclosure window, with the two statistical methods corroborating the direction over the full record but not pinning the split. And the connection-scaling test identifies what the demand side is physically doing: at about 230 VAr per connection added over 2013–2025, with no detectable connection-independent residual, from a term that sat on the inductive side of zero into the 2010s and has accumulated faster over the second half of the window than the first, the load fleet is not merely drawing fewer lagging vars overnight; its own standing shunt term is moving capacitive.

The defences, margins, and load models of power-system practice were built for lagging load and the undervoltage direction; the measured overnight flow has crossed to the other side, where no last-resort scheme is addressed to voltage rising and, in the plant-side loop, each protection operation reinforces the disturbance (Section VII); the same regime has produced two realised blackouts abroad, and the New Zealand system is already responding to it from both ends while its deeper demand-side driver remains unnamed in the rules. New Zealand's record—an advanced-state, small, isolated, heavily cabled analogue whose net-leading crossing preceded the 2025 European events by nearly a decade—is, to our knowledge, the longest direct measurement of that crossing. If the standing term is carried by the globally standardised product fleet, every system connected to the same supply chain is accumulating it on a similar schedule, at a dose set by its supply voltage (Section V-B)—on 230-volt systems roughly three times the North-American rate per device and four to five times the Japanese, so the dose ordering maps the exposure geographically and is itself the decisive comparative test, an ordering that places the lower-voltage fleets structurally later on the same accumulation, not exempt from it. Supply voltage sets the dose; transmission voltage sets its visibility. The term is created at the mains, indifferent to the network above it, while in any system-wide reactive account the boundary flow that would reveal it is dwarfed by the transmission network's own charging, which grows with the square of transmission voltage and with route length—so New Zealand's 220-kV maximum is an unusually transparent window, and in a 400-kV system that contrast is several times sharper (against 220 kV the voltage terms alone give $(400/220)^2 \approx 3.3$, and route length—which extra-high-voltage networks exist to span—widens it), where a network-side reading of the surplus is the natural one (the reading both 2025 investigations took, Section I-C). The claim is therefore priority of measurement, not of exposure: the failures arrived first where the network term is largest, not where the demand-side term is clearest. The systems with the most to gain from such a record are the ones without one: larger fleets, no measurement of the demand-side term, and, in Europe's case, a demonstrated failure mode.

The record also says where this goes. The drift shows no sign of slowing: the per-connection coefficient accumulated faster over the second half of the window than the first, was running at about 20 VAr per connection per year at the 2025 end, and the next device waves—an electric-vehicle charging and home-battery fleet expected to carry the largest input filters yet—are still arriving; nothing in the record yet marks the turn. Tracking that coefficient with a renewal model of device generations, and the decisive attribution measurement at a residential distribution transformer (Section V-C), are the nearest work (both detailed in Section VIII).

The stability question has moved with the sign: with overnight demand now net leading, defence design points at plant-side absorption—ride-through of absorbing plant, coordination of under-excitation limits on generators feeding capacitive networks [40]—and at solved network cases of the light-load state, which this boundary record cannot settle; and because the same V^2 scaling sets a network's own charging per kilometre, systems pairing extra-high-voltage networks with 230-volt fleets—Iberia's 400 kV among them—carry both terms at once. The prediction also runs the other way: unlike the passive filter fleet, the arriving wave of vehicle chargers, photovoltaic and battery inverters is controllable, and interconnection standards already define the response modes to steer it—IEEE Std 1547-2018 carries a voltage–reactive-power (volt-var) mode among its reactive-power controls and requires Category B resources to be capable of absorbing, as well as injecting, reactive power to at least 44% of nameplate apparent-power rating [51]. Large inverters operated, or required, to absorb at light load—running in the lagging quadrant against the fleet they share a board with—are then the natural first counter to the leading surplus at the grid exit point. Nearer the customer, the distribution networks the reverse flow transits hold two margins in records they already keep: tap-changer position histories—how much regulation headroom remains at light load—and the loss cost of the standing circulating current.

The limitations are stated throughout: the balanced panel controls churn but does not eliminate it; the decomposition attributes the drift, not a causal mechanism in any single load; the exact organic share and the level composition are not point-identified; the measurement gives the net standing term and not its inductive and capacitive limbs separately, so the device-level attribution of the connection-scaling term remains a labelled hypothesis for the capacitive limb, with its decisive low-voltage measurement identified; and a single national system is one observation—offset, not cured, by its position as a leading-edge analogue and by the two independent European corroborations. The defence-scheme and load-model development this measurement motivates is separate work. What this paper offers is the measured trajectory, its decomposition, the term it identifies, and the direction power-system analysis must now build for.

APPENDIX A
THE MEASUREMENT, NOT THE TREND

This appendix carries the measurement-error analysis summarised in Section II-C: the bound on the one error that does not average down, the timing argument for the 2010–2013 fleet replacement, and the test for a synchronous system-wide re-base.

A. The measurement chain, and what is documented of it

The quantity at risk is not the meter's arithmetic but the phase relationship presented to it. A grid-exit-point metering installation is a chain: current and voltage transformers on each phase, their secondary wiring and burden, and the meter. The meter end of that chain is well documented and tightly held— Class 0.2S for active energy, a certified Category-5 installation on a 36-month re-certification and 19-month inspection cycle—and the reactive class, though looser, is at least stated. The transformer end is neither.

The Code specifies the meter classes directly but takes the instrument transformers to their own standards: Schedule 10.1's table of standards for metering components lists the IEC 60044 series for current, inductive voltage, combined, capacitor-divider and electronic transformers, since superseded internationally by IEC 61869 [22]. It imposes no accuracy class of its own on them. Its one phase-displacement parameter, in the polyphase table, limits how far the phases of an installation may differ *from each other* (2°, irrespective of power factor); it says nothing about a displacement the phases share, which is precisely the component that survives averaging. Below that, three things are simply not in the public record: the class, ratio, burden and vintage of the transformers at any individual site; whether the overnight current at these points falls below the range over which the classes specify anything; and whether the 2010–2013 programme touched the transformers at all—the asset management plan that dates it records the replacement of the revenue *meters* [25].

Nor do the classes bind tightly where this paper looks. The IEC current-transformer classes specify accuracy only down to 5% of rated current—1% for the extended S classes—and permit three to four times the rated-current error at that bottom point [52]; the reactive meter class is specified only above 20% of rated current and gives no bound below it [22]. A metering chain at overnight minimum is therefore operating where its own specifications thin out, and the effect of a given phase displacement on the reactive reading is largest exactly there, since the overnight aggregate power factor sits near unity and the reactive component is small. This is why the term is bounded by assumption below, with the assumption made explicit and varied, rather than read off a documented class.

B. The bound on the phase-angle bias

Section II-C states the random-error case in full: class-bounded, bidirectional across 123 points and 29 years, it averages down and needs no more here. The systematic case deserves the full bound. A phase displacement β anywhere in the chain rotates the measured current phasor and injects a spurious reactive term of approximately $P \sin \beta$: proportional to the metered load, independent of the reactive power being measured, and concentrated in exactly the window this paper measures.

The limits above bind each chain independently, and the panel's 123 supply points carry several hundred separately specified transformer sets on their several hundred phases. Displacements enter with either sign and average down with the rest of the random budget; what does not average down is the *common-mode* part, the displacement every set shares. Suppose, generously, that this were half a degree across the whole panel. The spurious term is then about 0.9% of P—under 20 MVAr on the ≈1,900-MW overnight panel—a near-static offset roughly fifty times smaller than the measured 900-MVAr swing, and one that moves the crossing year by about half a year at most. Because the term scales with P, which grew by only about 280 MW over the record, it can contribute only about 0.1 MVAr/yr of apparent drift against the -31 MVAr/yr observed.

The result does not turn on the half degree. At three times it—1.5°, the order the classes themselves allow at the bottom of their specified range, applied coherently to every set—the offset is still under 50 MVAr, about an eighteenth of the swing, and the apparent drift about 0.26 MVAr/yr, two orders of magnitude below the measured rate.

In fact the magnitude does not matter at all, which is the stronger form of the argument. A *static* common-mode displacement generates apparent drift only through the growth of the load it multiplies, so the most it can generate across the record is $\Delta P \sin \beta$, and $\sin \beta \leq 1$. Overnight panel load grew about 280 MW. Even a physically absurd 90° displacement on every transformer set therefore falls short of the measured 900-MVAr swing by a factor of three. No static bias of any size reproduces this trajectory.

The phase-displacement route to the drift consequently requires β itself to move across the record—a drifting bias, not a fixed one—and three things work against that. Drift within the instruments is worked against by the re-certification and inspection cycle. A reset at the 2010–2013 meter replacement would enter as a step, and the series shows none. And the bias would have to move coherently across sites to survive averaging, which is the hypothesis the re-base test below examines directly and rejects. The phase-angle bias can therefore blur the *level* by tens of MVAr; it cannot manufacture the *drift*. Independently, no instrument error has reason to be cable-correlated (Section IV) or to scale with the connections behind each meter (Section V-C).

C. The 2010–2013 fleet replacement

The one metering transition in the record is bounded by its timing. The staggered 2010–2013 replacement of the legacy

PSI Quad4 instrumentation by four-quadrant ION8800A meters was an *upgrade* that improved the recording of leading (export) reactive power. Its possible bias is anchored at both ends of the record. At the 1997 anchor, leading flows were about 1% of overnight half-hours, so any under-recording of leading reactive power by the older fleet cannot materially bias the +466 MVAr starting point; the 2025 anchor sits wholly on the modern four-quadrant fleet, the instrumentation best able to measure the leading regime. The endpoint-to-endpoint swing is therefore insensitive to the upgrade, which could at most distort mid-period curvature—and in the conservative direction, since under-recorded leading reactive power would delay, not advance, the measured crossing. The upgrade also pre-dates the lagging-to-leading crossing (2016 on the demand panel, 2020 on the full panel), so the leading regime, the novel part of the claim, is observed wholly on the modern fleet. Directly on the data: the per-MW drift measured within the modern-fleet era alone (2014–2025) is -0.019 MVAr/MW/yr against -0.018 over the full record—if anything steeper—so the trend is not inherited from the older instrumentation.

D. Test for a system-wide metering re-base

The two arguments in Section III-B address gradual or staggered metering change. A single system-wide change is different: a one-date revision of sign convention or central processing would step every grid exit point in the same year and the same direction, a fingerprint no gradual physical trend leaves. We test for it (Fig. 8). Each grid exit point is first detrended by its own robust (Theil–Sen) line—robust so that a step, were one present, is not partially absorbed into a tilted least-squares fit and hidden—and the residuals are standardised by each site's own scatter; what remains is each site's wobble about its own path. Two per-year summaries are then taken across sites: the median residual (the "common wobble," near zero while wobbles are idiosyncratic, jumping only if sites move together) and the coherence, the share of sites on the same side of their own trend that year. Local causes cannot coordinate a hundred separate substations' deviations within a single year, but a central processing change would: a genuine re-base drives coherence toward 100%. An off-the-shelf change-point detector—which is forced to mark steps even on a smoothly bending curve, so its candidates are hypotheses rather than verdicts—flags years around 2002 and 2022; the earlier candidate abuts the 2000–2001 metering-vintage step flagged in Section III-B, and coherence at the candidates is only 67% and 69% against a typical-year 62%, indicating curve-bends rather than a coordinated re-base. The highest coherence anywhere, 75% in 2025, merely reflects most sites being leading together at the end of the record because the whole system has gone leading. No synchronous re-base underlies the trend.

Appendix B
The Mains Input Filter at 50 Hz

This appendix carries the component-level basis for the Section V-B hypothesis: what the electromagnetic-compatibility (EMC) filter is, why it is universal, and what it presents to the 50-Hz network.

A. Why the filter exists

A switched-mode supply chops current at tens to hundreds of kilohertz. Left unfiltered, that switching noise conducts back through the supply cord into the mains network. Conducted-emission limits (the international CISPR limits [30], covering roughly 150 kHz–30 MHz) are a condition of sale in most jurisdictions, New Zealand included, and the universal compliance solution is a passive low-pass filter at the appliance's own mains terminals.

The mandate's chronology brackets the measured record. The conducted-emission limit structure dates to CISPR 22:1985, absorbed by CISPR 32 in 2012 and applied in New Zealand as AS/NZS CISPR 32; New Zealand law has made compliance a condition of sale since at least 2001 (supplying non-compliant equipment is an infringement offence), lists switched-mode power supplies by name at the test-report conformity level, and—verified by full-text search of the current notice—contains no harmonic-current or power-factor requirement of any kind [33]. Regulatory force, too, predates the record: the European Union applied the harmonised EMC requirement from 1 January 1992 (Directive 89/336/EEC [34]) and permitted apparatus conforming to prior national regimes only until 31 December 1995 (Directive 92/31/EEC), so the directive's conformity route has been the sole lawful route to that market since 1996, carried through recasts to the current Directive 2014/30/EU, applying from 20 April 2016. A mandate that old cannot date the knee of Fig. 5B: what moved is the population beneath it. A wire-wound transformer needs no filter—the New Zealand notice leaves it at the lowest conformity level—so the mandate's standing capacitance arrived only as the switched-mode classes scaled through the 2000s and 2010s, wave by wave, on the schedule Section V-C's coefficient history measures.

On the exit side, external-power-supply no-load efficiency floors (California 2004; ENERGY STAR December 2004; United States statute for units manufactured from 1 July 2008, no-load $\leq$0.5 W [53]; the European Union staged to 0.30 W by April 2011; New Zealand's own mark III floor from 9 June 2011 [54]) made the iron-core linear supply progressively unsaleable, and the trans-Tasman regulator's own review records that international standards propagate to the New Zealand market through the global supply chain on a six-to-eight-year lag [55]. Applied to the rungs, that lag places the New Zealand shelf-stock conversion between about 2010—the earliest rung plus the shortest lag—and about 2019, the last rung plus the longest: a decade-long window that straddles the crossing of Fig. 5B rather than dating it. Only the last of these rungs was ever New Zealand law, which is why the conversion is read off the supply chain and not off the domestic instrument.

B. The circuit, and what 50 Hz sees

Fig. 9 shows the standard arrangement; the safety-class rationale for why the line-to-neutral *X-capacitors* are the one large element (metallised film, typically 0.1–2.2 μF, commonly one each side of the choke) is carried in Section V-B. The *common-mode choke* (two coupled windings on a shared core)

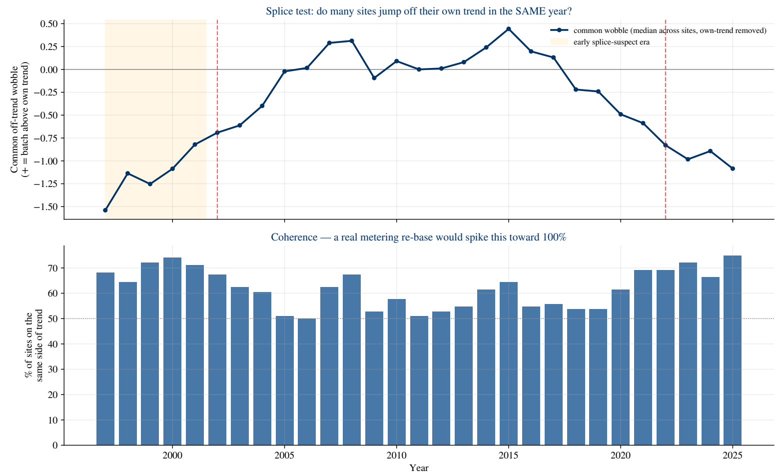

Fig. 8. Test for a system-wide metering re-base (the "splice" of the in-figure title: the join between metering eras). Each grid exit point is detrended by its own robust (Theil–Sen) line; the upper panel is the median residual across sites (the "common wobble") and the lower panel the coherence, the share of sites on the same side of their own trend each year. A genuine re-base would spike coherence toward 100% in a single year. The change-point candidate years (about 2002 and 2022, the dashed verticals) reach only 67% and 69% against a typical-year 62%: curve-bends, not a coordinated re-base.

presents high impedance to noise leaving on both conductors together and negligible impedance at 50 Hz; *Y-capacitors* (line-to-earth and neutral-to-earth) are held to nanofarads by touch-current limits and are electrically negligible here—where the appliance is earthed the line-to-earth element does inject at the fundamental, but at nanofarad scale that is under a per cent of the X-capacitor beside it, and the numerous small always-connected devices are double-insulated with no protective earth at all, so counting X alone biases the estimate very slightly low; a megohm-scale discharge resistor completes the set. At the fundamental the only material injection is therefore the X-capacitance, which draws pure leading current whenever the plug is live: $Q = \omega C V^2$, so at 230 V, 50 Hz, 0.1 μF injects 1.7 VAr, 0.47 μF injects 7.8 VAr, 1 μF injects 16.6 VAr, and 2.2 μF injects 36.6 VAr. Table V carries the census behind Section V-B's per-device figures—typical total class-X capacitance by device class, and the standing injection that capacitance draws on this mains and on North America's, where the same component earns a third of the reactive power. The two zero rows are as load-bearing as the populated ones: the sub-20-W charger swarm and the retrofit LED lamp contribute essentially nothing, which is why the standing term concentrates in the always-connected classes above about 25 W.

TABLE V
TYPICAL TOTAL LINE-TO-NEUTRAL (CLASS X) CAPACITANCE BY DEVICE CLASS, AND ITS STANDING INJECTION ON TWO MAINS

Device class	**X cap. (μF)**	**VAr, 230 V 50 Hz**	**VAr, 120 V 60 Hz**
USB charger $\leq$20 W	none found	$\approx$0	$\approx$0
LED retrofit lamp $\sim$5 W	not fitted	$\approx$0	$\approx$0
USB-PD and laptop supplies 27–65 W	0.10–0.22	1.7–3.7	0.5–1.2
Laptop and retail supplies 65–140 W	0.22–0.47	3.7–7.8	1.2–2.6
LED driver 12–100 W	0.066–0.45	1.1–7.5	0.4–2.4
TV / monitor supply 100–220 W	0.44–0.66	7.3–11.0	2.4–3.6
Desktop computer supply	0.37–1.8	6.1–29.9	2.0–9.8
Whiteware (laundry, inverter refrigeration)	0.47–1.41	7.8–23.4	2.6–7.7
Heat-pump / AC outdoor unit	1.41–2.0	23.4–33.2	7.7–10.9
Single-phase VSD input filter	0.94–4.2	15.6–69.8	5.1–22.8
Generic appliance filter, 1-ph	0.10–1.0	1.7–16.6	0.5–5.4

Capacitance ranges are design-grade: published reference designs with bills of materials, filter datasheets, and teardown reports, not measurements of shipped New Zealand product; both injection columns are computed from the capacitance column ($\omega C V^2$, assertion-checked in the replication set). Values are per device; PFC front ends and drives carry the multi-capacitor upper ends.

C. The aggregation asymmetry

The two capacitor classes are governed on opposite principles, and the contrast locates the regulatory gap precisely. The Y-capacitors' earth-leakage current is treated as what it is—a current that accumulates. It is budgeted per device: the touch-current allowance for ordinary plug-connected equipment is 3.5 mA, and design practice dimensions the Y-capacitance against that budget first [56]. It is budgeted again per installation: the United Kingdom's wiring regulations, for instance, require the accumulated protective-conductor current downstream of a residual-current device to be not more than 30 per cent of its rated residual operating current [32]. Filter datasheets print the consequence in their units, listing C_x in microfarads beside C_y in nanofarads. The X-capacitance's reactive current accumulates across devices in exactly the same way—the sum at a connection is tens of devices, at a grid exit point whole fleets—but no analogous budget exists at any scale: conducted-emission compliance is certified one device at a time against a standardised artificial mains network (CISPR 16-1-2), the harmonic-current standard is silent on fundamental reactive current (Section I-A), and we are not

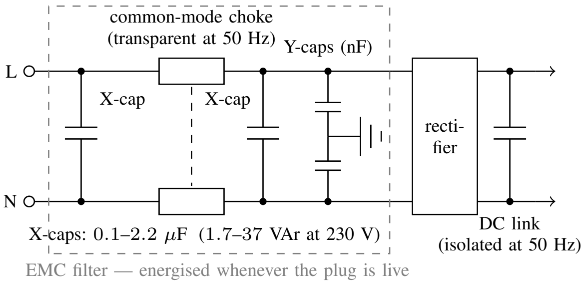

Fig. 9. The mains input stage of a switched-mode device. The EMC filter's X-capacitance sits directly across line and neutral, ahead of the rectifier and of any standby switching, and injects ωCV^2 of leading reactive power whenever the plug is live; the Y-capacitors are nanofarad-scale, and the large DC-link capacitor is isolated from the fundamental behind the rectifier. Component values are datasheet-grade typical ranges (Section V-B); on North America's 120 V, 60 Hz mains the same 0.1–2.2 μF range injects 0.5–12 VAr.

aware of any emission standard, wiring rule, or standards work item that has considered the aggregate. Where the regime recognised an aggregating current, it budgeted both the term and the sum; the standing reactive aggregate has never been anyone's design variable.

D. What does not count, and the grade of these values

The three capacitor classes that dominate a device's capacitance budget but contribute no standing fundamental-frequency injection—the DC-link electrolytic, motor-run capacitors, and a rooftop inverter's converter-side filter capacitors—and the one-way regulatory ratchet behind the accumulation are set out in Section V-B. The per-device values here are datasheet-grade, not bench-measured; the aggregate rests on Section V-B's labelled estimate; and the decisive measurement is the low-voltage one identified in Section V-C.

Reproducibility

Every number and figure in this paper is computed from public data (Electricity Authority grid metering and Commerce Commission information disclosures) in an accompanying set of analysis notebooks, which also document the path from the raw public records. Both input sets are public and published under CC BY 4.0—the grid metering on the Electricity Authority's Electricity Market Information platform, the network parameters in the Commerce Commission's information disclosures—and the archived package carries the inputs themselves together with the retrieval record and per-file checksums.

Acknowledgment

The author thanks colleagues at the Electricity Authority and Transpower for discussion of the reactive-power and voltage-management context, and the authors of the Rhodes autonomous-system studies for sharing corrected source material.

The author used Anthropic's Claude models as a research assistant throughout this work: literature searching, analysis and replication code, manuscript drafting and editing, and verification passes over numbers and citations. The research questions, analytical design, interpretation, and conclusions are the author's own. Every printed number is reproduced from public data by the accompanying notebooks and every citation was checked against its primary source; the author is responsible for all content.

References

[1] C. G. Kaloudas, L. F. Ochoa, B. Marshall, and S. Majithia, "Initial assessment of reactive power exchanges at UK grid supply points," in *Proc. CIRED Workshop 2014*, Rome, Italy, Jun. 2014, paper 0177.

[2] C. G. Kaloudas, L. F. Ochoa, B. Marshall, S. Majithia, and I. Fletcher, "Assessing the future trends of reactive power demand of distribution networks," *IEEE Transactions on Power Systems*, vol. 32, no. 6, pp. 4278–4288, Nov. 2017.

[3] RTE (Réseau de Transport d'Électricité), "Bilan de sûreté 2022," RTE, Paris-La Défense, France, Tech. Rep., Jul. 2023, sec. 5, pp. 26–27. Official English edition: *Reliability Report 2022*. [Online]. Available: https://assets.rte-france.com/prod/public/2023-07/2023-07-20-bilan-surete-2022.pdf

[4] Powerlink Queensland, "Managing voltages in South East Queensland," Powerlink Queensland, Project Assessment Conclusions Report, Sep. 2023. [Online]. Available: https://www.powerlink.com.au/sites/default/files/2023-09/Project%20Assessment%20Conclusions%20Report%20-%20Managing%20Voltages%20in%20South%20East%20Queensland.pdf

[5] M. Tazky, M. Regula, and A. Otcenasova, "Impact of changes in a distribution network nature on the capacitive reactive power flow into the transmission network in Slovakia," *Energies*, vol. 14, no. 17, p. 5321, 2021.

[6] J. Hannagan, R. Woszczeiko, T. Langstaff, W. Shen, and J. Rodwell, "The impact of household appliances and devices: Consider their reactive power and power factors," *Sustainability*, vol. 15, no. 1, p. 158, 2023.

[7] CIGRE Joint Working Group C4.24/CIRED, "Power quality and EMC issues with future electricity networks," CIGRE, Technical Brochure 719, 2018.

[8] Electric Power Research Institute, "Enhanced load modeling: Improved reactive power load modeling," EPRI, Palo Alto, CA, Technical Update 3002022354, Aug. 2021.

[9] International Electrotechnical Commission, "IEC 61000-3-2:2018+amd1:2020+amd2:2024 CSV electromagnetic compatibility (EMC) – part 3-2: Limits – limits for harmonic current emissions (equipment input current ≤16 A per phase)," IEC, Geneva, Switzerland, Tech. Rep., 2024, ed. 5.2 (Ed. 5.0 consolidated with AMD1:2020 and AMD2:2024).

[10] European Commission, "Commission regulation (EU) 2019/2020 of 1 october 2019 laying down ecodesign requirements for light sources and separate control gears," Official Journal of the European Union, L 315, Tech. Rep., 2019, cELEX 32019R2020. Annex II Table 4: minimum displacement factor $\cos\varphi_1$ for mains LED/OLED light sources above 5 W, measured at full load, applying from 1 September 2021; adopted into Australian law by the Greenhouse and Energy Minimum Standards (LED Lamps) Determination 2025, commencing 3 March 2026. New Zealand has no counterpart.

[11] ——, "Commission regulation (EU) 2016/1388 of 17 August 2016 establishing a network code on demand connection," Official Journal of the European Union, L 223, 18 Aug. 2016, pp. 10–54, 2016, eLI: http://data.europa.eu/eli/reg/2016/1388/oj.

[12] C. Vournas and T. Van Cutsem, "A review of overvoltage instability mechanisms," *Sustainable Energy, Grids and Networks*, vol. 47, p. 102475, 2026.

[13] A. H. Javed, P. H. Nguyen, J. Morren, and J. G. Slootweg, "Analyzing impact of capacitive reactive power flows at T-D interfaces," in *CIRED 2024 Vienna Workshop*. Vienna, Austria: Institution of Engineering and Technology, 2024, pp. 303–306.

[14] S. Baghban-Novin, M. Mahzouni-Sani, A. Hamidi, S. Golshannavaz, D. Nazarpour, and P. Siano, "Investigating the impacts of feeder reforming and distributed generation on reactive power demand of distribution networks," *Sustainable Energy, Grids and Networks*, vol. 22, p. 100350, 2020.

[15] A. Bosisio, F. Soldan, A. Morotti, G. Iannarelli, E. Bionda, and S. Grillo, "Lessons learned from Milan electric power distribution networks data analysis during COVID-19 pandemic," *Sustainable Energy, Grids and Networks*, vol. 31, p. 100755, 2022, also available as arXiv:2205.04894.

[16] ENTSO-E ICS Investigation Expert Panel, “Grid incident in Spain and Portugal on 28 April 2025 — final report,” European Network of Transmission System Operators for Electricity, Brussels, Belgium, Tech. Rep., Mar. 2026, published 20 March 2026. [Online]. Available: https://www.entsoe.eu/publications/blackout/28-april-2025-iberian-blackout/

[17] ——, “Grid incident in North Macedonia on 18 May 2025 — final report,” European Network of Transmission System Operators for Electricity, Brussels, Belgium, Tech. Rep., Apr. 2026, published 20 April 2026. [Online]. Available: https://eepublicdownloads.blob.core.windows.net/public-cdn-container/clean-documents/Reports/2026/ENTSO-E_250518_Final_Report_260420.pdf

[18] Australian Energy Market Operator, “Transmission connection point forecasting methodology,” Australian Energy Market Operator, Melbourne, Victoria, Australia, Tech. Rep., Jul. 2021, pp. 29–31: power factors at transmission connection points computed from historical active and reactive power over the top 1% of half-hour demand periods ranked by active power, with a leading/lagging label assigned on the sign of reactive power; non-inverter-based operational demand power factor assumed constant over the forecast horizon; footnote 23 anticipates power factor change at minimum demand and attributes it to inverter standards. Accessed 17 August 2026. [Online]. Available: https://www.aemo.com.au/-/media/files/electricity/nem/planning_and_forecasting/tcpf/2021-connection-point-forecasting-methodology.pdf

[19] D. Hume, “Power factors in the New Zealand power system,” in *Electricity Engineers’ Association (EEA) Conference*, Christchurch, New Zealand, Sep. 2025.

[20] Electricity Commission, “Electricity governance rules, part f (transport), section iii,” Electricity Commission, Wellington, New Zealand, Tech. Rep., Jan. 2008, rule 11.1 (Board to establish and maintain centralised data set): “The Board must establish and maintain a centralised data set”; rule 11.2 (Purpose of centralised data set). Print of 17 January 2008.

[21] ——, “Request for views on the centralised data set,” Electricity Commission, Wellington, New Zealand, Tech. Rep., Dec. 2004, prepared for the Electricity Commission by Partna Consulting Group. Proposed data list: “Half hourly GXP and GIP data dating back to 1 October 1996”, sourced from “the old ECNZ metering data storage files, MV90 metering data, and Avalon metering data”; reason for inclusion “Base information required for demand forecasting and assessment of market impacts of proposed investments”, and “a fundamental base data set for the Grid Investment Test”.

[22] Electricity Authority, “Electricity industry participation code 2010, part 10: Metering,” Electricity Authority of New Zealand, Wellington, New Zealand, Tech. Rep., 2025, consolidation as at 1 April 2025; cl 10.37(2)(a) and Schedule 10.1, Tables 1, 5, 6, and 7. [Online]. Available: https://www.ea.govt.nz/documents/7279/Part_10_-_Metering_-_1_April_2025.pdf

[23] International Electrotechnical Commission, “IEC 62053-22:2020 electricity metering equipment – particular requirements – part 22: Static meters for ac active energy (classes 0,1s, 0,2s and 0,5s),” IEC, Tech. Rep., 2020.

[24] ——, “IEC 61000-4-30 electromagnetic compatibility (emc) – part 4-30: Testing and measurement techniques – power quality measurement methods,” IEC, Tech. Rep., 2015.

[25] Transpower New Zealand, “Asset management plan,” Transpower New Zealand Limited, Tech. Rep., 2021, revenue metering replaced in RCP1 (2010–2013).

[26] ——, “Asset management plan,” Transpower New Zealand Limited, Tech. Rep., Apr. 2010, legacy PSI Quad4 revenue meters, installed from about 1994.

[27] International Electrotechnical Commission, “IEC 62053-23:2020 electricity metering equipment – particular requirements – part 23: Static meters for reactive energy (classes 2 and 3),” IEC, Tech. Rep., 2020.

[28] Institute of Electrical and Electronics Engineers, “IEEE std 1459-2010: IEEE standard definitions for the measurement of electric power quantities under sinusoidal, nonsinusoidal, balanced, or unbalanced conditions,” IEEE, New York, NY, USA, Tech. Rep., 2010, revised as IEEE Std 1459-2025.

[29] P. K. Sen, “Estimates of the regression coefficient based on Kendall’s tau,” *Journal of the American Statistical Association*, vol. 63, no. 324, pp. 1379–1389, 1968.

[30] International Special Committee on Radio Interference, “CISPR 32:2015+AMD1:2019 CSV, electromagnetic compatibility of multimedia equipment – emission requirements,” International Electrotechnical Commission, Geneva, Switzerland, Tech. Rep., 2019, edition 2.1, consolidated; first edition 2012, absorbing the scopes of CISPR 13 and CISPR 22. Applied in New Zealand as AS/NZS CISPR 32 under the Radiocommunications (EMC Standards) Notice 2019.

[31] International Electrotechnical Commission, “IEC 60384-14:2023, fixed capacitors for use in electronic equipment – part 14: Sectional specification – fixed capacitors for electromagnetic interference suppression and connection to the supply mains,” International Electrotechnical Commission, Geneva, Switzerland, Tech. Rep., 2023, edition 5.0; amended by AMD1:2025 (consolidated Ed. 5.1). Cited at the 2023 edition because that is the current sectional specification; note that IEC 60335-1:2020 still normatively cites the 2013+AMD1:2016 edition.

[32] Institution of Engineering and Technology and British Standards Institution, “BS 7671:2018, requirements for electrical installations (IET wiring regulations, 18th edition),” London, U.K., 2018, regulation 531.3.2: the accumulation of protective conductor currents downstream of a residual current device shall be not more than 30% of its rated residual operating current.

[33] Radio Spectrum Management, Ministry of Business, Innovation and Employment, “Radiocommunications (EMC standards) notice 2019,” New Zealand Gazette, notice 2019-go2372, 2019, in force 4 June 2019; prescribes AS/NZS CISPR 32 / CISPR 32 for multimedia equipment. Clause 7 assigns products incorporating switched-mode power supplies to level of conformity 2 (test report required); clause 6 assigns wire-wound mains-frequency transformers to level 1. Predecessor notices to 2004 carry the same assignment.

[34] Council of the European Communities, “Council directive 89/336/EEC of 3 may 1989 on the approximation of the laws of the Member States relating to electromagnetic compatibility,” Official Journal of the European Communities, L 139, 23 May 1989, 1989, provisions applied from 1 January 1992 (Art. 12); Directive 92/31/EEC permitted apparatus conforming to prior national regimes only until 31 December 1995. Recast as Directive 2004/108/EC, then Directive 2014/30/EU (applying from 20 April 2016).

[35] Environmental Health Intelligence New Zealand, “Home heating (indoor environment indicators),” Massey University indicator page, 2026, reporting Stats New Zealand Census data: heat pumps used in 47.3% (2018) and 66.8% (2023) of occupied private dwellings; accessed 7 August 2026. [Online]. Available: https://www.ehinz.ac.nz/indicators/indoor-environment/lack-of-home-heating/

[36] J. P. Ross and A. Meier, “Whole-house measurements of standby power consumption,” in *Proc. 2nd Int. Conf. on Energy Efficiency in Household Appliances and Lighting*, Naples, Italy, 2000, lawrence Berkeley National Laboratory LBNL-45967. Ten Californian homes, 190 standby appliances, mean 19 per household.

[37] C. Edlington, R. Ryan, M. Damnics, and L. Harrington, “Standby power in Australia: Measurement, policy and progress,” in *Proc. ACEEE Summer Study on Energy Efficiency in Buildings*, 2006, intrusive metering surveys: 61 homes and about 2,400 products (2000); 120 homes and about 8,000 appliances (2005). Products per household are derived from those totals, not stated by the authors.

[38] Electricity Authority, “Market share trends by root network supply point (NSP),” Electricity Market Information (EMI) market-structure dataset, 2026, monthly ICP counts by root NSP, December 2003–June 2026; retrieved 6 August 2026. [Online]. Available: https://www.emi.ea.govt.nz/Retail/Datasets/MarketStructure

[39] N. Isaacs, M. Camilleri, L. French, A. Pollard, K. Saville-Smith, R. Fraser, P. Rossouw, and J. Jowett, “Energy use in new zealand households: Report on the year 10 analysis for the household energy end-use project (HEEP),” BRANZ Ltd, Judgeford, New Zealand, Tech. Rep. Study Report SR 155, 2006, power factor measurements: §10; standby and baseload: §7.

[40] C. D. Vournas, V. C. Nikolaidis, and G. I. Tsourakis, “Coordinated countermeasures against overvoltage instability in autonomous power systems,” *IEEE Transactions on Power Delivery*, vol. 36, no. 6, pp. 3329–3338, Dec. 2021.

[41] G. N. Psarros, G. I. Tsourakis, and S. A. Papathanassiou, “Dimensioning of reactive power compensation in an autonomous island system,” *Applied Sciences*, vol. 12, no. 6, p. 2827, Mar. 2022.

[42] Transpower New Zealand (System Operator), “System security forecast 2022, part D: Power system security analysis — grid zone 2 (Auckland),” Transpower New Zealand Limited, Wellington, New Zealand, Tech. Rep., Dec. 2022, p. 12; the same passage appears in Grid Zone 1 (Northland), p. 11. [Online]. Available: https://static.transpower.co.nz/public/bulk-upload/documents/Part%20D%20GZ02%20Auckland.pdf

[43] ——, “N-1 thermal and voltage study — system security forecast 2024,” Transpower New Zealand Limited, Wellington, New Zealand, Tech. Rep., Jul. 2024, version 1, July 2024 (minor update June 2026),

p. 22. [Online]. Available: https://static.transpower.co.nz/public/bulk-upload/documents/N%20-%201%20Thermal%20and%20Voltage%20Study_Minor%20Update%202026%20June.pdf
[44] Transpower New Zealand, "Transmission planning report 2023," Transpower New Zealand Limited, Wellington, New Zealand, Tech. Rep., 2023, section 6.4.6, system condition SC6 (Lower North Island high voltages), printed p. 63. [Online]. Available: https://static.transpower.co.nz/public/uncontrolled_docs/Transmission%20Planning%20Report%202023.pdf
[45] Electricity Authority, "Electricity industry participation code 2010, schedule 12.6: Default transmission agreement template," Electricity Authority of New Zealand, Wellington, New Zealand, Tech. Rep., 2026, part 12, Schedule 12.6 (default transmission agreement template), Schedule 8 (Connection Code), cl 4.4 (Minimum power factor: unity or 0.95 lagging by region, during regional peak demand periods only); consolidation as at 1 July 2026.
[46] ——, "Electricity industry participation code 2010, part 8: Common quality," Electricity Authority of New Zealand, Wellington, New Zealand, Tech. Rep., 2026, cl 8.67(4)(a): kvar measured weekdays 0700–2100 only; consolidation as at 1 July 2026.
[47] Powerco Limited, "Electricity pricing policy fy26," Powerco Limited, New Plymouth, New Zealand, Tech. Rep., 2025, §15: per-kVAr charge only below 0.95 lagging.
[48] New Zealand Government, "Electricity (safety) regulations 2010 (SR 2010/36), regulation 28 (voltage supply to installations), as amended by SL 2025/225," New Zealand Parliamentary Counsel Office, Tech. Rep., 2025, reg. 7; $\pm 6\%$ to $\pm 10\%$, in force 13 November 2025. [Online]. Available: https://www.legislation.govt.nz/regulation/public/2010/0036/latest/DLM2763653.html
[49] WECC Modeling and Validation Subcommittee, "WECC composite load model specification," Western Electricity Coordinating Council, Salt Lake City, UT, USA, Tech. Rep., 2021, feeder reactive compensation Bfdr computed at initialisation "to balance the reactive consumption of the load devices and of the transformer and feeder with the load Q value specified in the power flow data"; on end-use protection operation the shunt capacitance is "tripped in proportion to the MW of each component tripped". Substation shunt Bss is held on load shedding. Every voltage trip parameter is undervoltage; the sole "high-voltage" occurrence is Tfixhs, a tap ratio. Text extracted and swept 23 Aug 2026; agrees with the April 2021 edition read for literature_review.md §C11a. [Online]. Available: https://www.wecc.org/sites/default/files/documents/meeting/2024/WECC%20Comp%20Load%20Model%20Specification_final.pdf
[50] C. Vournas and T. Van Cutsem, "On overvoltage instability," *Electric Power Systems Research*, vol. 262, p. 113589, 2027, available online 26 June 2026.
[51] Institute of Electrical and Electronics Engineers, "IEEE std 1547-2018: IEEE standard for interconnection and interoperability of distributed energy resources with associated electric power systems interfaces," IEEE, New York, NY, USA, Tech. Rep., 2018.
[52] Continental Control Systems, "Metering system accuracy," Continental Control Systems, LLC, Application Note AN-136, Apr. 2017, on the IEC 60044-1 / 61869-2 current-transformer classes: accuracy specified only to 5% of rated current (1% for the S classes), with three to four times the rated-current error permitted there. Available: https://ctlsys.com/wp-content/uploads/2017/04/AN-136-Metering-System-Accuracy-AppNote.pdf.
[53] United States Congress, "Energy independence and security act of 2007, public law 110–140, section 301 (External Power Supply Efficiency Standards)," 2007, 121 Stat. 1549. Class A external power supplies manufactured on or after 1 July 2008: no-load $\leq$0.5 W.
[54] New Zealand Government, "Energy efficiency (energy using products) regulations 2002 (SR 2002/9), schedule 1, as substituted by the energy efficiency (energy using products) amendment regulations 2011 (SR 2011/129)," New Zealand Parliamentary Counsel Office, Tech. Rep., 2011, reg. 4; external-power-supply MEPS (AS/NZS 4665.1/.2), in force 9 June 2011.
[55] Energy Efficiency and Conservation Authority, "Consultation regulation impact statement: External power supplies," EECA, for the trans-Tasman E3 programme, Wellington, New Zealand, Tech. Rep., 2025. [Online]. Available: https://www.eeca.govt.nz/assets/EECA-Resources/Consultation-Papers/Consultation-Regulation-Impact-Statement-External-Power-Supplies-2025.pdf
[56] Würth Elektronik eiSos, "Application note ANP015: 1-phase line filter design," Waldenburg, Germany, 2024, touch-current allowance for common applications with protective conductors: 3.5 mA; Y-capacitance dimensioned against the leakage budget first, with X2 values often 10 to 100 times larger than Y2.